Brain Struct Funct (2013) 218:1569–1589
DOI 10.1007/s00429-012-0478-2

ORIGINAL ARTICLE

The structure of Pavlovian fear conditioning in the amygdala

Hadley C. Bergstrom · Craig G. McDonald · Smita Dey · Haying Tang · Reed G. Selwyn · Luke R. Johnson

Received: 8 May 2012 / Accepted: 25 October 2012 / Published online: 20 November 2012

Abstract Do different brains forming a specific memory allocate the same groups of neurons to encode it? One way to test this question is to map neurons encoding the same memory and quantitatively compare their locations across individual brains. In a previous study, we used this strategy to uncover a common topography of neurons in the dorsolateral amygdala (LAd) that expressed a learning-induced and plasticity-related kinase (p42/44 mitogen-activated protein kinase; pMAPK), following auditory Pavlovian fear conditioning. In this series of experiments, we extend our initial findings to ask to what extent this functional topography depends upon intrinsic neuronal structure. We first showed that the majority (87 %) of pMAPK expression in the lateral amygdala was restricted to principal-type neurons. Next, we verified a neuroanatomical reference point for amygdala alignment using in vivo magnetic resonance imaging and in vitro morphometrics. We then determined that the topography of neurons encoding auditory fear conditioning was not exclusively governed by principal neuron cytoarchitecture. These data suggest that functional patterning of neurons undergoing plasticity in the amygdala following Pavlovian fear conditioning is specific to memory formation itself. Further, the spatial allocation of activated neurons in the LAd was specific to cued (auditory), but not contextual, fear conditioning. Spatial analyses conducted at another coronal plane revealed another spatial map unique to fear conditioning, providing additional evidence that the functional topography of fear memory storing cells in the LAd is non-random and stable. Overall, these data provide evidence for a spatial organizing principle governing the functional allocation of fear memory in the amygdala.

Keywords Lateral amygdala · Basal amygdala · Lateral ventricle · Network · Neural circuit · Fear · Fear learning · Memory · Mitogen-activated protein kinase (MAPK) · Calcium calmodulin-dependent protein kinase II (CAMKII) · Magnetic resonance imaging (MRI) · Principal components analysis (PCA) · Multiple discriminant analysis (MDA) · Multivariate ANOVA (MANOVA) · Dual-labeling immunofluorescence · Sprague–Dawley rat · Consolidation · Cytoarchitecture · Principal cell-type · Mapping · Micro anatomy · Stability · Topography · Organization

Electronic supplementary material The online version of this article (doi:10.1007/s00429-012-0478-2) contains supplementary material, which is available to authorized users.

H. C. Bergstrom · L. R. Johnson (✉)
Department of Psychiatry, School of Medicine, Uniformed Services University (USU), Bethesda, MD 20814, USA
e-mail: lukejohnsonphd@gmail.com

C. G. McDonald
Department of Psychology, George Mason University, Fairfax, VA, USA

S. Dey · H. Tang · R. G. Selwyn · L. R. Johnson
Center for Neuroscience and Regenerative Medicine (CNRM), School of Medicine, Uniformed Services University (USU), Bethesda, MD 20814, USA

H. Tang · R. G. Selwyn
Department of Radiology, Uniformed Services University (USU), School of Medicine, Bethesda, MD, USA

L. R. Johnson
Program in Neuroscience, School of Medicine, Uniformed Services University (USU), Bethesda, MD 20814, USA

L. R. Johnson
Center for the Study of Traumatic Stress (CSTS), School of Medicine, Uniformed Services University (USU), Bethesda, MD 20814, USA

Introduction

The amygdala is generally considered to play a key role in Pavlovian fear conditioning (Quirk et al. 1995; Davis 1992; Pape and Pare 2010; LeDoux et al. 1990a; Fanselow and LeDoux 1999; Maren and Fanselow 1996; Johnson and Ledoux 2004). Within the amygdala, only a sparse subset of neurons has been found to encode any given fear memory (Han et al. 2007, 2009; Reijmers et al. 2007; Rumpel et al. 2005; Nomura et al. 2011; Bergstrom et al. 2011). Despite significant progress localizing fear memory to neuronal subsets in the amygdala (i.e., the fear engram), very little work has addressed the basic organizing principles of the engram. Specifically, one unresolved question is how fear memory encoding neurons in the amygdala are spatially allocated. Even less is known about the relative stability of their locations across different brains. Knowledge about the spatial allocation of neurons encoding memory across individuals is a key step toward understanding the basic organizing principles of the engram, both at the functional and anatomical level.

We previously studied these questions by mapping the topography of activated neurons in the dorsolateral amygdala (LAd) following Pavlovian fear conditioning, for a specific tone and shock paring. We uncovered a consistent pattern of activated neurons in those animals encoding a Pavlovian conditioned fear memory (Bergstrom et al. 2011). This finding suggests that neurons in the LAd, activated as a result of Pavlovian fear conditioning, form a spatially organized functional topography. However, the degree to which this organization is dependent upon the intrinsic neuronal cytoarchitecture of the LAd or is a property of memory formation itself is not known. Resolving the interdependence of functional versus intrinsic neuronal organization represents a significant technical challenge, because the amygdala is a nucleated structure without a clearly defined cytoarchitecture (Pitkänen 2000; McDonald 2003). Lesion and pharmacological studies suggest that fear memory encoding likely involves neurons from both the dorsoventral and rostrocaudal axis of the amygdala (Nader et al. 2001; Wilensky et al. 1999). Whether any additional amygdala subnuclei, outside of the LAd, possess topographically organized fear memory encoding maps is unknown. Finally, how contextual fear conditioning is spatially allocated in the amygdala is also not understood.

The objectives of the current study were to first, evaluate the spatial organization of neurons encoding Pavlovian fear conditioning throughout the LA and B subnuclei of the amygdala; second, to measure the activated neuronal distribution at another rostrocaudal location; third, to map the functional organization of neurons encoding auditory cued or contextual fear memory; fourth, to control for intrinsic principal neuron density which may skew the interpretation of functional maps. Neurons involved in the formation of fear conditioning in the amygdala were identified using immunohistochemistry for phosphorylated (p44/42) mitogen-activated protein kinase (pMAPK) (Schafe et al. 1999, 2000, 2008; Duvarci et al. 2005; Herry et al. 2006; Davis and Laroche 2006). To maximize the accuracy of statistical comparisons across individual brains, neurons expressing pMAPK following cued (auditory) and contextual fear conditioning were mapped at a narrow, quantitatively aligned coronal plane. Principal component analysis (PCA) was applied to the data set to visualize and interpret spatial patterns. Although it is well established that the expression of pMAPK in the amygdala is necessary for lasting fear memory storage, the presence of pMAPK is not entirely restricted to associative learning (Schafe et al. 1999, 2000, 2008; Bergstrom et al. 2011). In these experiments, we asked if there were any locations within the LA or B where neurons specific to CS and US associations were consistently located. We hypothesized that cued and contextual fear memory formation would activate a unique and stable spatial pattern of neurons and that these spatial maps would be a function of memory formation itself, rather than amygdala cytoarchitecture.

Materials and methods

Animals

All procedures were conducted in accordance with the National Institute of Health *Guide for the Care and Use of Experimental Animals* and were approved by the Uniformed Services University Institutional Animal Care and Use Committee. Male Sprague–Dawley rats (Taconic) weighing 225–250 g on arrival were group housed (2/cage) on a 12-h light:dark cycle with food and water provided without restriction. Rats were allowed at least 7 days of acclimation to the colony and handled on 3 days prior to testing. All rats weighed 322.6 ± 9 g at time of testing. Rats ($N = 50$) were subdivided into two experimental (Paired $n = 12$ and Shock alone $n = 11$) and two control group (Unpaired $n = 10$ and Box alone $n = 10$). Following fear conditioning, rats were subdivided into two groups of study: an anatomy (Paired $n = 7$, Unpaired $n = 5$, Shock alone $n = 6$ and Box alone $n = 7$) and behavior (Paired $n = 5$, Unpaired $n = 5$, Shock alone $n = 5$ and Box alone $n = 3$) group. Separate cohorts were used for CaMKII immunohistochemistry ($n = 4$), magnetic resonance imaging (MRI) ($n = 1$) and dual-labeling immunofluorescence ($n = 2$).

Pavlovian auditory fear conditioning

Rats were habituated to the fear conditioning chamber (Context A) for 30 min 1 day prior to conditioning. On training day, rats were placed in Context A for fear conditioning. Context A consisted of a Plexiglas rodent conditioning chamber and metal grid floor (Coulbourn Instruments, Lehigh Valley, PA, USA). The chamber was dimly illuminated by a single house light (2–3 lux) and enclosed within a sound-attenuating chamber (background dB = 55). The chamber was cleaned between testing runs with a 70 % EtOH solution and thoroughly dried. Prior to presentation of the stimuli, rats were left to explore the chamber for 3 min. The Paired group was presented with five pairings of an auditory CS (5 kHz, 75 dB, 20 s) that co-terminated with a foot shock US (1.0 mA, 500 ms). The Unpaired group received five non-overlapping presentations of the CS and US (145 s mean intertrial interval). The contextual fear conditioning group (Shock alone) was presented with five USs (without the auditory CS). The Box-alone group was exposed to the fear conditioning chamber for the same duration as the experimental group but without presentation of a discrete US or CS. Animals were removed from the chamber 60 s following the final stimulus presentation. Rats in the behavioral groups were placed back into the fear conditioning chamber (Context A) 24 h following training for analysis of freezing to the original training context (contextual fear memory). Three days following testing for contextual memory, rats were placed into a novel context (Context B) and presented with ten auditory CSs alone (auditory fear memory test). Context B consisted of plastic flooring covered with fresh bedding, altered geometry and spatial cues (red and black tape) relative to context A and 1 % acetic acid solution served as a novel odorant and cleaning agent. An experimenter who was blind to the experimental condition of the animals scored freezing behavior from digitized videos. Freezing behavior is widely considered a measure of conditioned fear. Freezing was defined as the absence of all movements except those related to respiration (Fanselow 1980). For the auditory CS test, freezing was scored only during the CS presentations (20 s) and for the contextual test, freezing was sampled for 20 s in 40-s fixed intervals for 10 m. Freezing was also scored during the 3-min time period prior to the presentation of the auditory CS to evaluate the level of non-specific or generalized freezing to the novel chamber (Context B). A mean freezing value was calculated from the ten scored freezing episodes and transformed into a percent freezing by dividing the total freezing time by the number of scored freezing episodes and dividing by 100. Mean percentage freezing was the dependent variable for all behavioral statistical analyses.

Immunohistochemistry

In the adult brain, learning-induced synaptic plasticity requires activity in the extracellular signal-regulated/mitogen-activated protein kinase (ERK/MAPK) pathway (Sweatt 2001; Thomas and Huganir 2004). Pavlovian fear conditioning is dependent upon and detectable as an increase in phosphorylated MAPK (pMAPK) in the LA (Schafe et al. 1999, 2000, 2008). Thus the presence of pMAPK in neurons in the amygdala following fear conditioning is a molecular signature of fear memory formation. In the second (anatomy) cohort, we mapped neurons immuno-positive for pMAPK ($pMAPK^+$) from the right LA and B amygdala nuclei following auditory Pavlovian fear conditioning.

Tissue preparation

Rats were anesthetized for perfusion exactly 60 min following auditory fear conditioning (Schafe et al. 2000). Rats were anesthetized with an intraperitoneal (i.p.) injection of a ketamine/xylazine (100 mg/kg, 10 mg/kg) cocktail and transcardially perfused through the ascending aorta with ice-cold saline followed by ice-cold 4 % paraformaldehyde/1 % glutaraldehyde/0.1 M phosphate buffer (PB) at pH 7.4 (250 mL). For calcium calmodulin-dependent protein kinase II (CaMKII) immunocytochemistry and dual-labeling immunofluorescence, glutaraldehyde was not included in the fixative. Brains were removed and stored in the fixative overnight (4 °C), then stored in phosphate buffered saline (PBS) for no more than 3 days. Free-floating sequential coronal brain sections containing the amygdala were cut on a vibratome at 40 μm. All sections were treated with 1 % sodium borohydride and washed (PBS) prior to processing for pMAPK immunoreactivity.

pMAPK immunoperoxidase reactions

Sections were first blocked in PBS containing 1 % bovine serum albumin (BSA) for 1 h. Next, sections were incubated in a rabbit polyclonal antibody to phospho-p44/42 MAPK (Thr202/Tyr204, 1:250 dilution, Cell Signaling Technology, Boston, MA) in PBS–1 % BSA for 24 h at room temperature. Following washing (PBS), slices for pMAPK immunoreactivity were subsequently incubated with biotinylated goat anti-rabbit IgG (1:200 dilution, Vector Laboratories, Burlingame, CA, USA) in PBS–1 % BSA for 30 m. Slices were then washed (PBS) again and incubated in avidin–biotin HRP complex (ABC Elite, Vector Laboratories, Burlingame, CA, USA). After a final wash (PBS), activated neurons were developed in SG chromagen (Vector Laboratories, Burlingame, CA, USA). Serial sections were mounted in numerical order on

gelatin-subbed slides and air-dried then dehydrated in a graded series of alcohol, xylene and coverslipped.

Dual-labeling immunofluorescence

One possible anatomical explanation for spatial organization among functionally active neurons is that the pattern reflects the intrinsic cytoarchitecture of the amygdala, rather than a property of memory formation per se. To address this question, we first set out to determine the predominant cell type that expresses pMAPK at its peak following fear learning. We targeted principal neurons, because they comprise the majority (80–85 %) of the neuronal population in the LA and B nuclei (McDonald 1984). To detect principal neurons, a monoclonal antibody to the alpha subunit of calcium calmodulin-dependent protein kinase II (CaMKII) was used as a marker (McDonald et al. 2002).

For dual-labeling immunofluorescence experiments, all rats ($n = 2$) underwent fear conditioning using parameters identical to those described above. Sections containing the whole amygdala from Bregma −2.04 through −3.60 were first blocked in PBS containing 1 % BSA and 0.02 % Triton X-100 for 1 h. Next, sections were incubated in a cocktail of two primary antibodies: a rabbit anti-pMAPK antibody (1:250, Cell Signaling Technology, Boston, MA, USA) and a mouse anti-αCaMKII (1:500, clone 6D193, Santa Cruz Biotechnology, Santa Cruz, CA, USA) in PBS/1 % BSA/0.02 % Triton X-100 overnight at room temperature. Following washing in PBS, slices were subsequently incubated in the dark in species-appropriate Alexa Fluor 488 antibodies (to visualize CaMKII antibody) and Alexa Fluor 594 antibodies (to visualize pMAPK antibody) raised in goat (1:200 dilution, Life Technologies, Carlsbad, CA, USA). Sections were then washed in PBS, mounted on gel-coated glass slides using Vectashield mounting medium (Vector Laboratories, Burlingame, CA, USA) and stored at 4 °C until analysis. In a parallel experiment, the primary antibodies were excluded separately. No staining was found, confirming the signal was due to the presence of primary antibody (data not shown). In another parallel experiment, the secondary antibodies were excluded separately. These analyses confirmed the specificity of the secondary antibodies (data not shown). Dual-stained neurons were visualized using a fluorescent microscope (Olympus BX61). Immunofluorescence analysis was conducted by counting Alexa Fluor 488 fluorescence (CaMKII) and Alexa Fluor 594 fluorescence (pMAPK). To avoid issues with a lack of penetration for the primary antibodies, neurons were counted from the top and bottom of each section where staining quality was optimal.

CaMKII immunoperoxidase reactions

Based on the experiments described above, we used CaMKII immunohistochemistry for mapping principal neurons. To avoid putative differences in CaMKII expression levels as a result of fear conditioning, rats in the CaMKII group ($n = 4$) did not undergo fear conditioning training prior to killing. Sections containing the amygdala were matched at the entrance to the LV (Bregma −3.36; see below) so that a direct comparison could be made between CAMKII and pMAPK immunoreactive neurons. Following the blocking step identical to that described above, sections were incubated overnight at room temperature in a mouse monoclonal antibody to the alpha subunit of CaMKII (20 μg/mL, clone 6G9, Millipore, Billerica, MA, USA) in PBS–1 % BSA. Slices were washed (PBS) and then incubated in biotinylated goat anti-mouse IgG (1:200, Vector Laboratories, Burlingame, CA, USA) in PBS–1 % BSA for 30 m. Subsequent processing steps were identical to those described above.

Section alignment

Spatial analysis across different brains requires precise stereotaxic alignment. To align different brains, we first used high-resolution MRI on a single brain to identify an anatomical structure in vivo that fulfilled the following requirements: it (1) was readily identifiable, (2) was amygdala-centric, and (3) possessed a rapid change in morphology from rostral to caudal.

In vivo MRI morphometry of the lateral ventricle

One female Sprague–Dawley rat weighing 326.8 g was used for neuroimaging. Gender differences in the morphometry of the brain at the spatial resolution of our analysis (100 × 100 × 200 μm) were not expected. During scanning, the rat was anesthetized using isoflurane (1.5–2 %) and maintained at a constant body temperature. All MR images were acquired using a 7.05 T Bruker BioSpec imaging system (Bruker Biospin, Inc., Billerica, MA, USA) with a 20-cm horizontal inner-bore diameter and dedicated rat brain phased-array ($n = 4$) head coil.

To locate an anatomical reference point that fulfilled the aforementioned criteria, multiple horizontal anatomical images were acquired using a two-dimensional (2D) multi-slice spin-echo T_2-weighted sequence with repetition time (TR) of 12 s and echo time (TE) of 72 ms. The image matrix was 256 × 256 with an in-plane resolution of 0.1 mm × 0.1 mm, slice thickness of 1.0 mm and 0.5 mm inter-slice gap. T_2-weighted anatomical images provided optimal contrast to identify the lateral ventricle (LV) as an amygdala-centric reference point. The horizontal slice also

served as a reference for the location of the LV for the subsequent coronal MR acquisition. Coronal anatomical images were obtained at the LV using a 2D multi-slice spin-echo T_2-weighted sequence with TR of 12 s and TE of 72 ms. The image matrix was 256 × 256 with an in-plane resolution of 0.1 mm × 0.1 mm, slice thickness of 0.5 and 0.1 mm inter-slice gap. Three sets of scans were acquired with a 0.2 mm offset and interleaved, yielding a distance of 0.2 mm between slices through the LV to visualize the rapid change in morphology of the LV. Total imaging time was ~25 min for each scan. For the analysis of the area of the LV, we used high-resolution in vivo 3D fast spin-echo MR imaging to achieve a more accurate measure of LV area. The parameters for 3D MR imaging were TR of 2 s, TE of 72 ms and the field of view was 25.6 × 25.6 × 6.4 mm^3 which provided an in-plane resolution of 0.1 × 0.1 × 0.2 mm with no inter-slice gap. The 3D T_2-weighted anatomical images provided sufficient contrast to delineate the LV for an area measurement. Region of interest (ROI) analysis on the LV was used for quantification purposes. The slope was calculated between the first and second slice by determining the change in the area (mm^2) of the LV divided by the slice thickness (0.2 mm). The slope calculation was used as a morphometric parameter to estimate the "steepness" of change in size of the LV from rostral to caudal.

In vitro morphometry of the lateral ventricle

To quantitatively match sections for spatial analysis across brains, the morphology of the LV was digitally reconstructed (Neurolucida, MBF Biosciences, VT, USA) from five consecutive sections (−3.32 to −3.48 Bregma) in immunohistochemical-processed tissue. The area of the LV was calculated (NeuroExplorer, MBF Biosciences, VT) and sections across brains matched based on LV area. The LV area over the distance of five consecutive 40 μm sections (200 μm) was used to calculate the slope. Slopes calculations derived from in vitro (histology) and in vivo (MR imaging) measurements of the LV were compared to assure that the rapid change in shape of the LV was not an artifact of immunohistochemical processing.

Cell counts

All sections were matched using the entrance to the LV as an anatomical landmark. Cell counting was conducted at three locations, −3.24 to −3.44 mm posterior to Bregma (Paxinos and Watson 2007). At this coronal level, all of the LA and B subnuclei are well represented. Cell counts from consecutive sections were not included in the analysis and, thus, it was not necessary to correct for double-counting. For all neuronal counting, the experimenter was blind to experimental condition. The anatomical boundaries of the various amygdala nuclei were partitioned at 2× magnification using a contour-tracing tool (Neurolucida, MBF Biosciences, VT, USA) superimposed onto a digital image of the amygdala from a rat brain atlas (Paxinos and Watson 2007) at the appropriate Bregma coordinate. Therefore, the dimensions of the contour were identical between experimental groups. At the rostrocaudal level selected for analysis, the following subdivisions were chosen for quantitative analysis: LA nuclei, dorsal (LAd), ventromedial (LAvm), ventrolateral (LAvl) and B nuclei, anterior (BLa), posterior (BLp). The basal ventrolateral (BLV) nucleus was not included into the analysis due to overall low number of $CaMKII^+$ and $pMAPK^+$ neurons and low variability for this region. The (*XYZ*) coordinates of individually labeled pMAPK neurons within the LA were marked under a 20×/0.5 NA objective. Markers (*XYZ* coordinates) and contours were quantified (NeuroExplorer, MBF Biosciences, VT, USA). The mean density of $pMAPK^+$ neurons within the surface area was calculated as the ratio between the total number of $pMAPK^+$ neurons and the contour area (mm^2) of each nucleus from three sections (Bregma −3.24 to −3.44).

Multiple discriminant analysis (MDA)

A standard multivariate analysis of variance (MANOVA) was first used to determine the statistical relationship among amygdala nuclei encoding fear conditioning. A significant value for the conservative Pillai's Trace test statistic was followed up by one-way ANOVAs on each amygdala subnuclei. Next, MDA was applied to the data set to determine the relative contribution of each nucleus to the overall difference in $pMAPK^+$ neuron density. MDA is a classification method that finds an optimal combination of variables (a dimension) that discriminates the groups. A set of canonical variate correlation coefficients (loading values) represents the relative contribution of each variable to the extracted dimension. In this way, MDA was used to determine how relative $pMAPK^+$ density across a combination of amygdala nuclei contributed to overall difference between learning conditions. For MDA, the grouping variable was the experimental conditions and the independent variables (discriminate variates) were the amygdala subnuclei (LAd, LAvm, LAvl, BLa, BLp, BLv). The analysis was based on a within-groups covariance matrix. Because group sizes were unequal, we based prior probabilities on the group size. Box's test was used to determine the equality of covariance matrices. To gain insight into the relationship between the experimental conditions (independent variables) and the pattern of $pMAPK^+$ expression across amygdala subnuclei (discriminant variates), we examined the structure matrix which contains

the canonical variate correlation coefficients (Supplemental Table 1).

Heat maps

Heat maps aid the visualization of neuronal density across a sampling area. Importantly, in this study, heat maps were used to verify results from the PCA (described below). To build the heat maps, *XY* coordinates for individual neurons were binned (OriginLab, Northampton, MA, USA). The bin dimensions were calculated by the sampling area and the mean number of $pMAPK^+$ neurons (n) for all subjects, where (D) is twice the expected frequency of points in a random distribution (de Smith et al. 2009): $D = (\text{area}/n)2$. Neurons that fell into each bin were counted and saved into a matrix. Values within each bin were assigned a color for visualization purposes (a "heat" map) (SigmaPlot v 12, Systat Software, San Jose CA, USA).

Principal components analysis (PCA)

Pavlovian fear conditioning activates a complex, non-uniform population of neurons in the amygdala (Schafe et al. 2000; Bergstrom et al. 2011). The complexity of memory allocation in neural networks makes finding spatial patterns based on visual inspection alone difficult. To find and summarize patterns, we used a PCA-based approach. PCA is a commonly used unbiased technique for reducing highly dimensional data sets into a smaller set of components that reflect patterns of covariance (Jolliffe 2002; Bergstrom et al. 2008). PCA always finds patterns (components) of variance within a data set, assuming that variance exists. The goal of this study was selecting the principal component(s), if any, described a functionally relevant pattern of activated neurons related to the learning conditions. We then verified the pattern using quantitative and qualitative methods.

To conduct PCA, the various amygdala subnuclei were each partitioned into a matrix using the same methods described above for generating the heat maps. We used this approach so that direct comparisons could be made between the statistical patterns extracted by PCA and the natural pattern of activated neurons. Another advantage to this approach was that the geometry of the matrix was determined by *XY* coordinates of neurons mapped within the boundaries of the contour, rather than a priori matrix construction. Bins for the LAd measured 115 μm^2 (40 bins), LAvm 140 μm^2 (26 bins), LAvl 150 μm^2 (17 bins), BLa 135 μm^2 (36 bins). Each bin represented the total number of neurons contained within the 40-μm-thick section. Thus, each bin represented the *XYZ* axes (115 × 115 × 40 μm). The total number of activated neurons corresponding with each bin in the matrix was considered the dependent variable in the PCA. The BLp was not included into the PCA due to the overall low number of neurons, and the fact that the density of $pMAPK^+$ neurons in the BLp was not significantly different between groups and that the BLp did not contribute significantly to the overall variance between groups as determined by MDA.

A covariance matrix PCA was chosen to generate a more defined component structure. The covariance matrix represents all of the possible covariance values from all the different dimensions. To make the pattern of loadings more pronounced, simple and interpretable, components were rotated (promax, kappa 2). The result of PCA is set of component loadings and scores.

Component loadings

Loadings reflect the pattern of variability associated with a particular component. The magnitude of the loading value for each of the variables indicates its relative contribution to the component structure. We used the loading values from the pattern matrix for pattern visualization. The pattern matrix was interpreted because it contains more information about the unique contribution of a variable to a component. For pattern visualization, loading values were assigned to a loading matrix (loading map) and color was applied according to a frequency distribution. The loading maps for each component were compared to the raw and mean neuronal density heat maps with the goal of verifying the results of the PCA.

Component scores

Scores indicate the "strength" or "relatedness" of a particular pattern associated with each subject. We grouped component scores by experimental condition (Paired, Unpaired, Shock alone and Box alone) and statistically compared them across all the respective components (MANOVA). This technique was helpful in verifying which extracted component(s) were associated with the learning conditions (see above for details on the MANOVA). Following a significant test statistic (Pillai's trace), each score was independently compared between conditions. To avoid spurious conclusions resulting from multiple comparisons, α was set at α/n for each comparison (Bonferroni correction). Subsequent post-hoc analysis was performed using a Bonferroni corrected t test.

Outliers

Principal components analysis is sensitive to outliers (Jolliffe 2002). Subjects with scores (Z scores) that fell outside ±3 for the extracted component accounting for the greatest

variance were designated outliers. If outliers were present we reran the PCA with outliers omitted.

PCA reliability

We used several independent tests to verify the reliability of the PCA in finding meaningful patterns. First, we statistically compared scores for all components using MANOVA. Second, we evaluated (*t* test with Bonferroni correction) the bins that loaded the highest and lowest for the component that accounted for the greatest variance associated with the experimental learning conditions. Third, we visually compared the loading matrices for all components with the topographic heat maps. Fourth, we mapped an additional section and correlated the PCA results within-subjects.

Statistical analysis

Unless otherwise noted, all group comparisons were conducted using one-way ANOVA followed by a Bonferroni corrected post-hoc test. Correlations were calculated using Pearson's *r*. All values embedded in the text are expressed as the mean ± standard error of the mean. *P* values at or below 0.05 were considered statistically significant. All statistical analyses were conducted using SPSS v19 software (IBM Corporation, Armonk NY, USA).

Results

Pavlovian fear conditioning

Twenty-four hours following the acquisition of Pavlovian fear conditioning, rats in the Paired (freezing response was 90 %), Unpaired (79 %) and Shock alone (71 %) behavioral conditions exhibited equivalently high freezing when placed back into the original training environment (context A) compared with the Box alone (20.5 %) control group (one-way ANOVA, $F[3, 14] = 11.3$; $p = 0.001$). This result indicates the formation of a contextual fear memory. Three days following the contextual fear memory test, presentation of the auditory CS in a novel environment (context B) resulted in a robust freezing response in the Paired (96 %) relative to Unpaired (34 %), Shock alone (12 %) and Box alone (3 %) conditions (one-way ANOVA, $F[3, 14] = 32.3$; $p = 0.000002$). This result indicates that the fear conditioning protocol employed was sufficient to induce a long-term fear memory that was specific to the association of the tone and shock (Fig. 1). There was no statistical difference in pre-CS freezing (one-way ANOVA; $p = 0.42$) indicated that memory reactivation 3 days following acquisition was specific to the auditory CS.

pMAPK$^+$ neuron density across LA and B nuclei

How the combination of neurons located across LA and B nuclei interacts to contribute to the acquisition of Pavlovian fear conditioning remains largely unknown. To address this question, we first visualized the distribution of activated neurons by generating high spatial resolution (140 μm^2) density maps. Density maps revealed variability in the distribution of neurons immuno-positive for pMAPK labeling (pMAPK$^+$) across the LA and B nuclei after Paired fear conditioning and control conditions (Fig. 2). Next, we applied multivariate analysis of variance (MANOVA) to the density of pMAPK$^+$ cells located across five nuclei of the amygdala (LAd, LAvm, LAvl, BLa, BLp). Using Pillai's trace, there was a significant effect of the

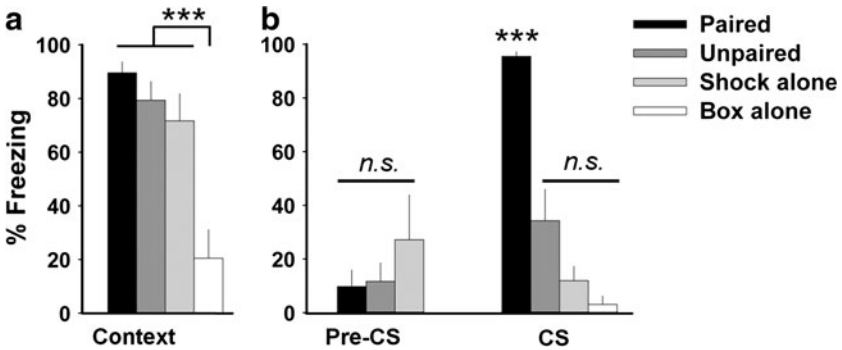

Fig. 1 Freezing to the auditory CS in a novel environment was restricted to Paired fear conditioning. **a** Rats presented with the US in the fear conditioning chamber showed a robust freezing response when returned to the same chamber 24 h later, indicating the formation of a contextual fear memory. **b** Presentation of the CS in a novel environment 3 days following the contextual fear memory test resulted in a significantly greater freezing response in the Paired (96 %) relative to the Unpaired (34 %), Shock alone (12 %) and Box alone (3 %) conditions. Freezing prior to the presentation of the auditory CS in the novel environment (pre-CS) was low for all conditions, indicating that the freezing response for the Paired group was specific to the auditory CS. *Triple asterisk* denotes a statistically significant difference ($p < 0.001$)

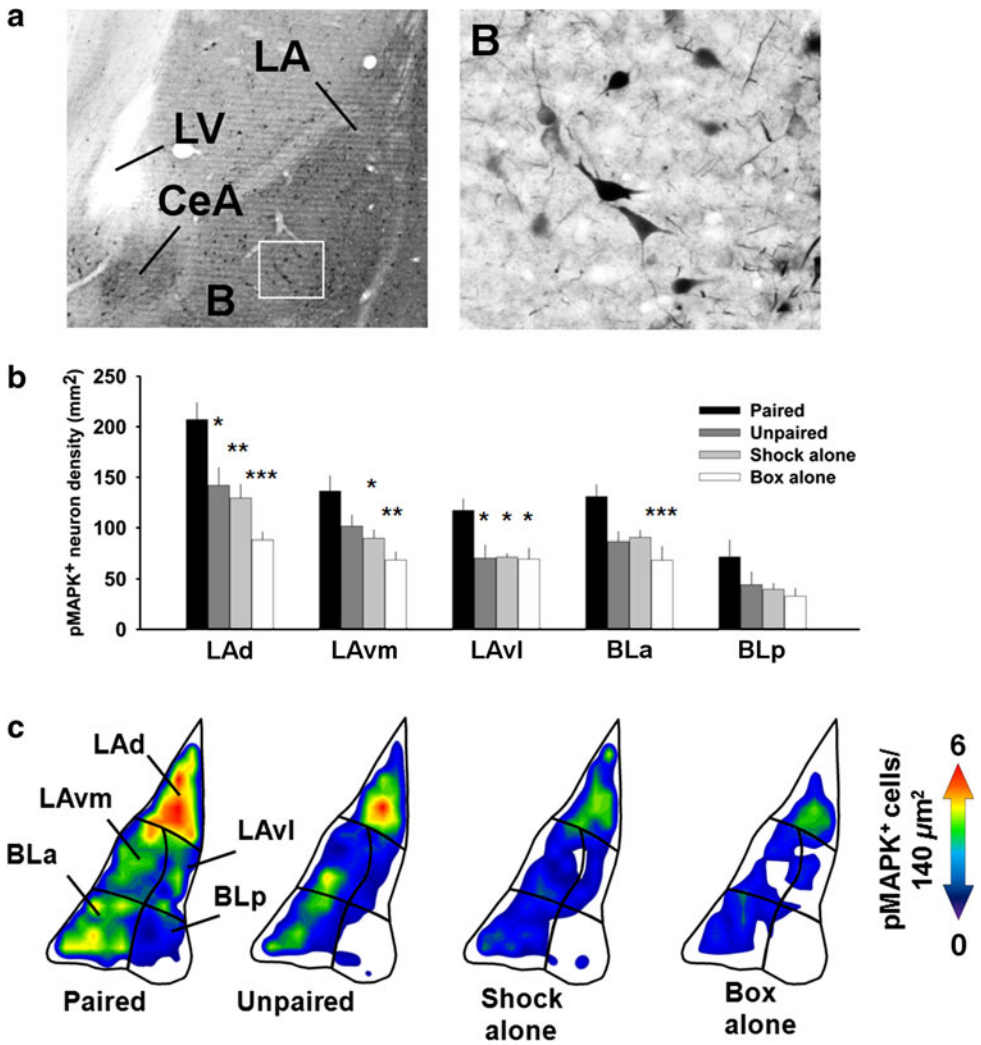

Fig. 2 Paired auditory fear conditioning was accompanied by a greater density of pMAPK$^+$ neurons in the LA and B nuclei. **a** Representative photomicrograph of a pMAPK immunohistochemical-processed section showing the various subnuclei of the amygdala and pMAPK$^+$ neurons at 4X (*left panel*) and ×20 (*right panel*) magnification. **b** The activation pattern for pMAPK$^+$ neurons in the Paired condition was widely distributed across LA and B nuclei (Multivariate ANOVA with Bonferroni post hoc). In the LAd and LAvl only, there was greater pMAPK$^+$ density in the Paired relative to the Unpaired condition, suggesting a unique contribution of the LAd and LAvl to the encoding of fear memories specific to auditory CS–US pairing. **c** Density "heat" maps of the LA and B nuclei depicting the distribution of pMAPK$^+$ cells in the Paired, Unpaired, Shock alone and Box alone conditions. The spatial resolution for the density maps was 140 μm^2. The *colors* for each bin reflect as estimation of the mean spatial density from low (*blue*) to high (*red*). (LAd) dorsolateral amygdala, (LAvm) ventromedial amygdala, (LAvl) ventrolateral amygdala, (BLa) anterior basolateral amygdala, (BLp) posterior basolateral amygdala, (CeA) central nucleus of the amygdala, (LV) lateral ventricle, (LA) lateral amygdala, (B) basal amygdala. *$p < 0.05$, **$p < 0.01$, ***$p < 0.001$ statistical difference relative to the Paired condition

experimental conditions on the density of pMAPK$^+$ neurons across amygdala nuclei ($V = 0.98$, $F(15, 57) = 1.85$; $p = 0.05$. Significant differences in pMAPK$^+$ neuron density across experimental conditions were found for the LAd (one-way ANOVA, $F[3, 21] = 13.7$; $p = 0.00003$), LAvm ($F[3, 21] = 6.8$; $p = 0.002$), LAvl ($F[3, 21] = 5.3$; $p = 0.007$), BLa ($F[3, 21] = 5.9$; $p = 0.004$), but not BLp ($p = 0.10$). We then used MDA to determine the relative contribution of each amygdala nucleus to the overall difference in pMAPK$^+$ density between experimental conditions. Results of MDA showed the first discriminant function segregated the groups $\Lambda = 0.217$, $X^2(15) = 29.8$; $p = 0.013$, but the second ($p = 0.65$) and third ($p = 0.80$) did not. This result indicates that a single underlying pattern in the density of pMAPK$^+$ neurons across the LA and B nuclei discriminated the experimental conditions.

LAd

The relative pattern of pMAPK$^+$ neurons across amygdala nuclei is reflected in the loading values (canonical variate correlation coefficients) resulting from MDA (Supplemental

results). The loading values for discriminant function 1 revealed that the LAd contributed most to the overall difference in the pattern of pMAPK$^+$ neuron density between experimental conditions, followed by the LAvm, BLa, LAvl and BLp (Supplemental results). This finding was confirmed by a Bonferroni post-hoc test showing that the density of pMAPK in the LAd was greatest in the Paired relative to Unpaired ($p = 0.05$), Shock alone ($p = 0.005$) and Box alone ($p = 0.00002$) conditions. There were no significant differences in the density of pMAPK neurons among the Shock alone and control conditions. Together these results confirm others (Maren and Quirk 2004; Johnson et al. 2008; Radley et al. 2007; Repa et al. 2001; Nader et al. 2001; Lamprecht and LeDoux 2004) indicating the LAd as an important site for neuronal plasticity associated with the formation of auditory fear memories.

LAvl

In addition to the LAd, the density of pMAPK$^+$ neurons in the LAvl was greater in the Paired group compared to the Unpaired (Bonferroni post hoc, $p = 0.049$), Shock alone ($p = 0.031$) and Box alone ($p = 0.015$) groups. This result indicates a unique contribution of the LAvl to the encoding of fear memories specific to auditory CS–US pairing. Anatomically localized activation of neurons in the LAvl following fear conditioning has been previously reported using other markers of cellular activity, including pMAPK (Schafe et al. 2000) and c-fos (Wilson and Murphy 2009; Trogrlic et al. 2011).

LAvm

In the LAvm, the density of pMAPK$^+$ neurons was greater in the Paired relative to Shock alone (Bonferroni post hoc, $p = 0.048$) and Box alone conditions ($p = 0.01$), but was not different from the Unpaired condition.

BLa

In the BLa, the density of pMAPK$^+$ neurons was significantly greater in the Paired relative to Box alone condition only (Bonferroni post hoc, $p = 0.003$). There was no difference in the density of pMAPK$^+$ neurons in the Paired, Unpaired and Shock alone conditions for the BLa. Taken together, results from the LAvm and BLa subnuclei indicate a degree of non-specificity for pMAPK$^+$ neurons following Pavlovian auditory fear conditioning.

Contextual fear conditioning and pMAPK in the amygdala

The density of pMAPK$^+$ neurons in those that received unsignaled foot shocks (Shock alone) and in the Unpaired group was equivalent to those that experienced the conditioning chamber alone without presentation of the US (Box alone) in both LA and B nuclei. However, rats in the Shock alone and Unpaired conditions exhibited a high freezing behavior when re-exposed to the environment previous associated with the foot shock (Fig. 1), indicating the formation of a contextual fear memory. Therefore, these results suggest that contextual fear conditioning was not associated with elevation in the number of pMAPK$^+$ neurons in the LA and B nuclei of the amygdala, a finding previously reported in the LA only (Schafe et al. 2000).

Overall, multivariate analyses across LA and B nuclei revealed a predominance of pMAPK$^+$ neurons following conditioned fear for auditory stimuli relative to contextual and control conditions. The activation pattern for pMAPK$^+$ neurons in the Paired condition could best be described as widely distributed in the LA and B nuclei (Fig. 2). However, as clearly visualized in the density maps (Fig. 2) and distinguished by multivariate analysis, the LAd was the greatest contributor to the overall difference between experimental conditions in the pattern of pMAPK$^+$ neuron density across amygdala nuclei. In addition to the LAd, a greater density of pMAPK$^+$ neurons for the Paired group compared to all control conditions, including the Unpaired group, was anatomically localized to the LAvl. These results indicate the LAvl as another locus for neurons specific to encoding auditory fear conditioning. The importance of the LAvl subnucleus in associative fear conditioning has been previously reported using a different molecular marker (Trogrlic et al. 2011; Wilson and Murphy 2009).

Section alignment using in vivo high-resolution MRI and in vitro morphometrics

We used high-resolution MRI to help locating an anatomical structure in vivo that could serve as a landmark for section alignment. A visual inspection of T_2-weighted horizontal and coronal MR images clearly shows the lateral ventricle (LV) in close proximity to the amygdala (amygdala-centric). The area of the LV was quantified from manually drawn ROIs on 3D coronal T_2-weighted MRI slices. Quantitative analysis (slope) confirmed a rapid change in morphology of the LV from the rostral to caudal axis (Fig. 3). A rapid rostral-caudal change in the LV area allows for quantitative section alignment.

To quantitatively match sections for spatial analysis across brains, the morphology of the LV was reconstructed (Neurolucida, MBF Biosciences, VT, USA) from five consecutive sections (−3.36 to −3.48 Bregma) in immunohistochemical-processed tissue. The area of the LV was calculated (NeuroExplorer, MBF Biosciences, VT, USA) and sections matched based on the LV area. The mean area

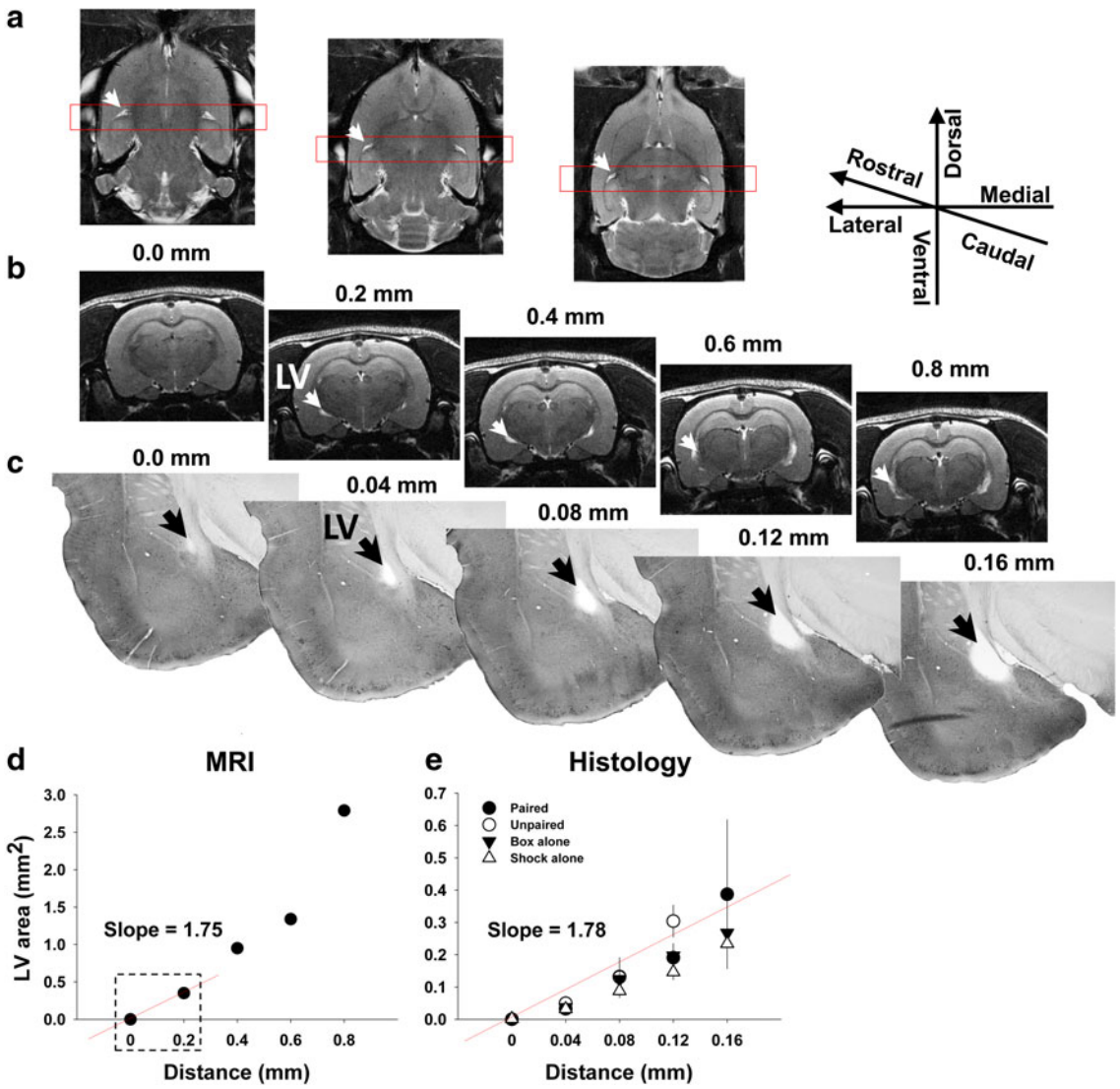

Fig. 3 Identification of the lateral ventricle as an anatomical reference point with in vivo 7 T MRI and in vitro quantitative section matching. **a** Horizontal T_2-weighted MR images from ventral to dorsal depicting the lateral ventricle (LV) (*arrowhead*) in vivo and an approximation of the region of interest (ROI) (*red box*) for T_2-weighted coronal MR slices. **b** Coronal T_2-weighted MR images through the LV depicting the rapid change in morphology of LV (*arrowheads*). **c** Representative photomicrograph of five consecutive 40 μm immunohistochemical-processed sections depicting the progressive and rapid change in the morphology of the LV in vitro (*arrowheads*). LV shows the section used for section alignment at the approximate Bregma coordinate for spatial analysis (−3.36). **d** ROI analysis showing the rapid increase in the area of the LV across 3D T_2-weighted MR images. The *red line* indicates where the values used for the calculation of slope for the initial opening of the LV were derived. **e** The area (mm^2) of the LV was closely aligned at the section chosen for mapping of amygdala neurons (approx. −3.36 Bregma). The *red line* indicates the slope from −3.32 to −3.48

of the LV between Paired (0.033 ± 0.011 mm^2), Unpaired (0.049 ± 0.022 mm^2), Shock alone (0.031 ± 0.005 mm^2) and Box alone groups (0.037 ± 0.008 mm^2) was not significantly different at −3.36 Bregma (one-way ANOVA; $p = 0.74$). In addition, the variance for the mean LV area for all groups at −3.36 Bregma was far lower (801.5 mm^2) than that at −3.4 (9,850.0 mm^2), −3.44 (7,799.5 mm^2) and −3.48 (56,193.1 mm^2) Bregma, providing verification that the section chosen for mapping was closely aligned between experimental conditions. In addition, the slope calculation for the LV area from Bregma −3.32 to −3.48 in vitro (slope = 1.78) was nearly identical to the slope obtained from quantification of the LV in MR images in vivo (slope = 1.75). Therefore, the results from MRI verified that the rapid change in the morphology of the LV identified in immunohistochemical-processed sections was not an artifact of tissue processing. We conclude the section used for spatial analysis was precisely aligned at a quantifiable anatomical landmark—the entrance to the lateral amygdala (Fig. 3). Overall, a number of factors

made the LV a useful anatomical reference point for stereotaxic alignment of the rat brain, including: (1) the close proximity of the LV to the amygdala, (2) the ease at which the LV can be identified in both histology and MRI T_2-weighted images, (3) the rapid change in morphology from rostral to caudal, and (4) the low variance for the area of the LV entrance between different brains (Fig. 3).

PCA on the spatial distribution of pMAPK$^+$ neurons

LAd

Principal components analysis was conducted on 25 subjects (from all four conditions) and 40 bins (1,288 neurons) from the LAd (Paired 79 ± 7.7; Unpaired 54.2 ± 6.9; Shock 45.2 ± 6.1; Box alone 34 ± 2.5 see Fig. 4). PCA extracted ten spatial components (SCs). All SC scores were statistically compared between conditions (MANOVA). Using Pillai's trace, there was a significant effect of condition on the PCA scores ($V = 1.72$, $F(30, 42) = 1.88$; $p = 0.03$). Subsequent comparisons (Bonferroni corrected) of all SCs revealed only one SC (SC1) whose factor score differed significantly among conditions (one-way ANOVA, $F[3, 21] = 17.7$; $p = 0.000006$). The loading values for SC1 corresponded with the difference in spatial distribution of pMAPK$^+$ neurons across experimental conditions, as depicted by the density maps (Fig. 5). This result confirms that a stable spatial organization of pMAPK$^+$ neurons distinguished the experimental conditions (Bergstrom et al. 2011). A statistical comparison of the scores for the remaining SCs (2–10) failed to yield another spatial component that could account for any other source of variability in the spatial distribution of pMAPK$^+$ neurons between experimental conditions. This result provides an important verification that no other underlying spatial dimension could account for variability in the distribution of pMAPK$^+$ neurons across experimental conditions. A subsequent Bonferroni post-hoc test on the scores for SC1 revealed significantly greater scores for subjects in the Paired group relative to those in the Unpaired ($p = 0.0002$), Shock ($p = 0.00004$) and Box-alone ($p = 0.00002$) conditions. There were no significant differences detected between any combination of the Unpaired, Shock-alone and Box-alone conditions. This result indicates that the spatial pattern of pMAPK$^+$ neurons extracted in SC1 was unique to Paired auditory fear conditioning. Together, these results from PCA suggest a stable topography of pMAPK$^+$ neurons that was specific to fear conditioning for auditory stimuli. Stability in the spatial pattern of functionally active neurons across individuals suggests that neurons that encoded Pavlovian fear conditioning are spatially organized. In addition, a lack of statistical significance between SC scores for the Shock-alone condition indicates that contextual fear conditioning was not

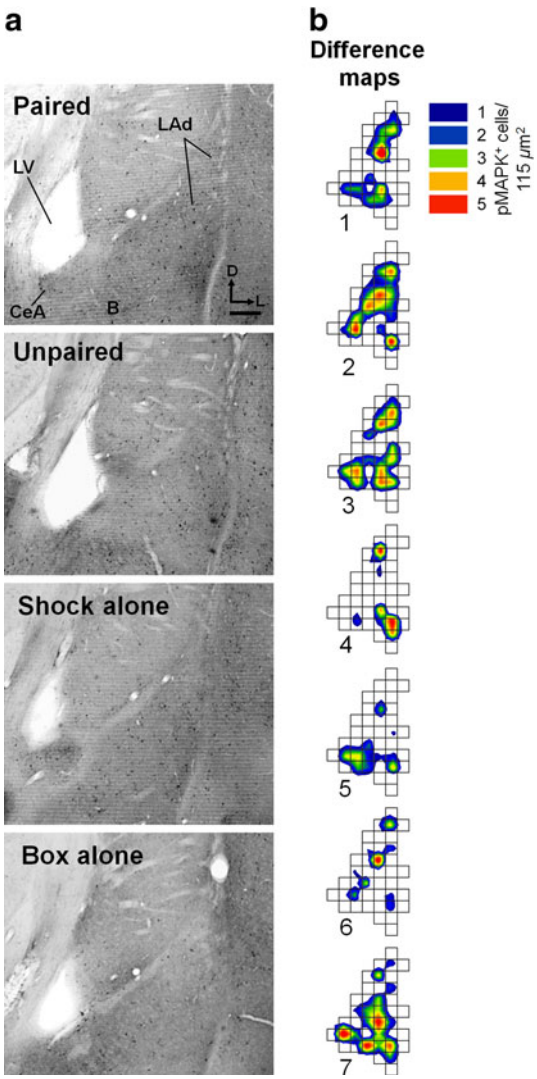

Fig. 4 Difference heat maps for individual subjects. **a** Representative photomicrographs depicting pMAPK immunohistochemical-processed sections from the dorsal portion of the amygdala at ×4 magnification for the Paired, Unpaired, Shock alone and Box alone conditions. *Scale bar* represents 150 μm. **b** Density heat maps estimating the difference in the spatial density of pMAPK neurons for individual subjects in the Paired group minus the mean of activated neurons from the Unpaired conditioning. The matrix overlay provides scale (115 μm^2) (LV) Lateral ventricle, (LAd) Dorsolateral amygdala, (B) Basal amygdala, (CeA) Central nucleus of the amygdala

associated with a spatial organization of pMAPK$^+$ neurons in the LAd. To visualize how the SC scores from individual subjects for the first two SC were distributed among the experimental conditions, we projected them onto a two-dimensional axis (Fig. 5).

pMAPK$^+$ neurons in the LAd form a functional map

Principal components analysis captured a unique pattern (SC1) of pMAPK$^+$ neurons in the LAd that was stable

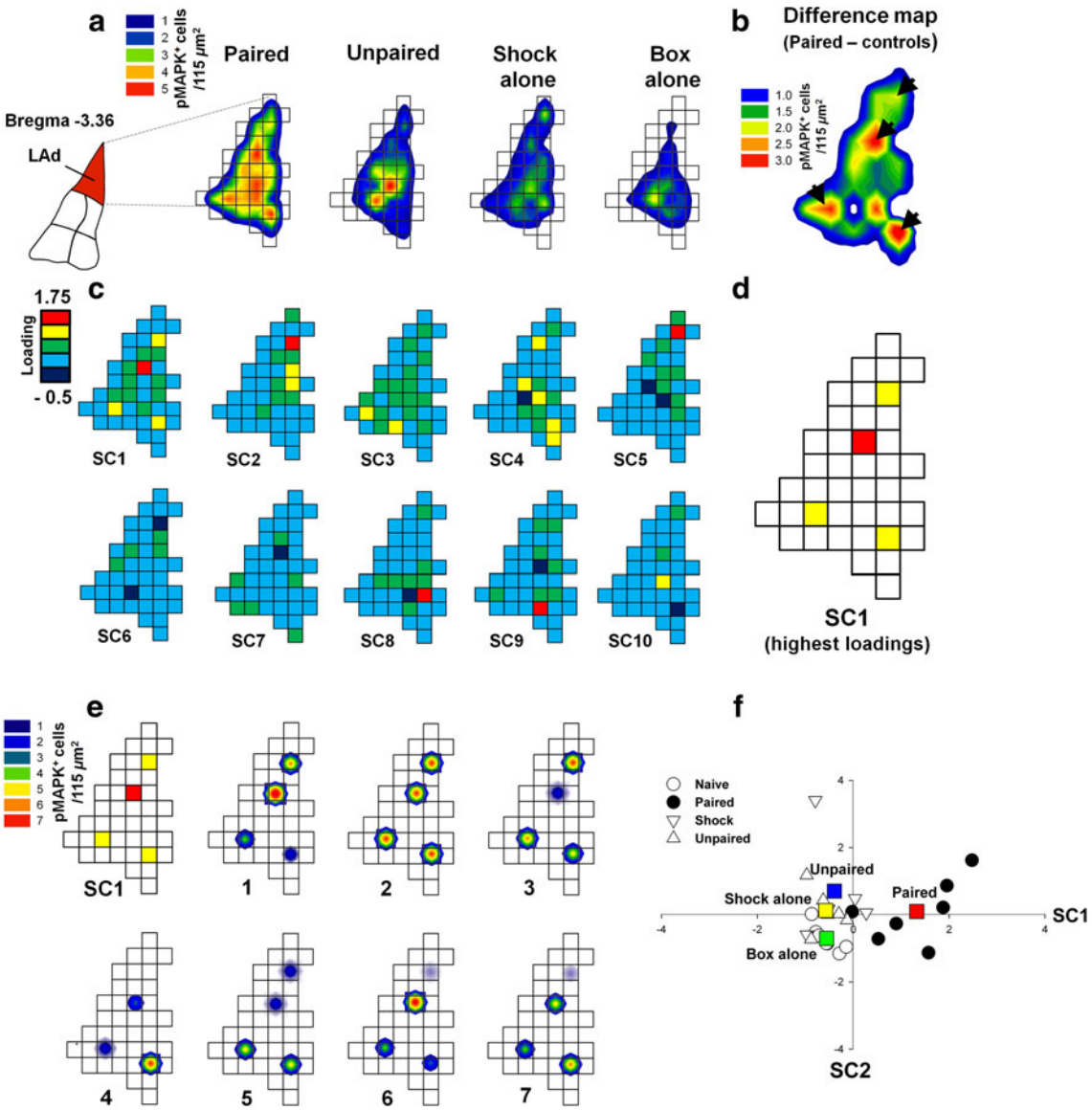

Fig. 5 PCA revealed a stable topography of neurons in the LAd that was unique to the encoding of an auditory fear memory. **a** Depiction of the spatial resolution and geometry of the matrix used in generating the density "heat" maps and for PCA on the LAd. The spatial resolution of the heat maps and the loading matrix was identical (115 μm^2). **b** A difference map showing the mean number of pMAPK$^+$ neurons in the Paired group minus the mean number of activated neurons across all control conditions. The *arrowheads* indicate regions of greatest difference that corresponded with SC1. **c** PCA extracted ten spatial components (SCs). Of the ten SCs extracted by PCA, the pattern of loading values associated with SC1 best discriminated the most prominent difference in the spatial distribution pMAPK$^+$ neurons between experimental conditions. **d** The bins with the highest loading values (top 10 %) were highlighted for visualization purposes. **e** The total number of neurons contained within the bins that loaded highest on SC1 was mapped to visualize the stability of the pattern across individual subjects in the Paired group. **f** To illustrate how the spatial components segregated the conditions along the first two spatial components (SC1 and SC2), we projected the SC scores for individual subjects onto a 2D axis. The SC1 scores for the Paired condition were significant different from the Unpaired ($p = 0.0002$), Shock-alone ($p = 0.00004$) and Box-alone ($p = 0.00002$) conditions, indicating that SC1 represents a pattern of pMAPK$^+$ neurons that was specific to brains encoding auditory Pavlovian fear conditioning

across brains that had acquired auditory fear conditioning. What distinguished the distribution of pMAPK-labeled neurons in the LAd was selective activation of neurons in discrete regions of the superior and inferior LAd, an observation consistent with the pattern of loading values for SC1 (Fig. 5). The difference between experimental conditions, as reflected by the loading values, can be attributed to the pattern of pMAPK$^+$ neurons in the Paired condition since higher SC scores were found for the Paired versus all other experimental conditions (Fig. 5). The spatial pattern of pMAPK$^+$ neurons associated with SC1 was independently confirmed by statistically comparing the

number of pMAPK$^+$ neurons between experimental conditions for bins with the most prominent loading values (multiple comparison analysis; Supplemental results). Results indicated that the bins with the highest loading values also contained a significantly greater number of pMAPK$^+$ neurons (*Top* 10 %; Bin 13, $p = 0.02$; Bin 27, $p = 0.0008$; Bin 36, $p = 0.0008$; Bin 7, $p = 0.012$ Bonferroni corrected p values) that were uniquely activated following auditory fear conditioning (Supplemental results and Supplemental figure 1). The fact that bins with the highest loading values were also the regions of greatest difference in pMAPK$^+$ neuron number between experimental conditions further confirms the use of PCA in extracting meaningful patterns of variance associated with the experimental manipulation (Bergstrom et al. 2011). We also compared neuron number between conditions in bins that loaded the lowest on SC1 (Bottom 10 %; Bin 28, 30, 17, 25). These additional comparisons were conducted to provide another test of the reliability of the PCA. No significant differences were found for the bins that loaded the lowest on SC1 (one-way ANOVA; Bin 28, $p = 0.41$; Bin 30, $p = 0.43$; Bin 17, $p = 0.23$; Bin 25, $p = 0.35$ uncorrected p values) (Supplemental results). This result, together with the result of the previous multiple comparisons test, confirms the reliability of the PCA to extract patterns related to the learning conditions. The PCA was also useful for revealing regions of co-activation across experimental groups (Fig. 5). Overall, PCA revealed that the distinguishing feature in the topography of pMAPK$^+$ neurons for the Paired group was a greater density of pMAPK$^+$ neurons that was localized to discrete regions of the superior and inferior LAd (Fig. 5), a finding that confirms previous work (Bergstrom et al. 2011).

PCA was conducted on the remaining four nuclei of the amygdala. There were no other spatial components extracted by PCA that discriminated a spatial pattern of pMAPK$^+$ neurons that was unique between experimental conditions. This result indicates that systematic spatial patterning of pMAPK$^+$ neurons following the acquisition of Pavlovian fear conditioning was anatomically restricted to the LAd.

Degree of plasticity in micro regions of the LAd

Our next analysis sought to provide initial quantitative measures for how much plasticity (change in pMAPK$^+$ neurons), as a result of CS and US pairing, occurred in the bins with the highest loading values. Relative to the Unpaired group, we estimate that 37 % of neurons encoding CS and US pairings were localized to four bins, which represented 10 % of the total area analyzed (Fig. 5). This estimate is conservative, as it is based on neurons only from bins with the highest loading values. When comparing plasticity between Paired and Unpaired groups for all bins (less the four highest loading value bins) the change in neuron number was 40 %. In contrast, when comparing plasticity, between Paired and Unpaired groups, in the four highest loading value bins, the change in neuron number was 157 %. These values further emphasize the effectiveness of the PCA in identifying micro regions of plasticity following associative conditioning. Moreover, these values provide quantitative estimates for the degree of plasticity in specified micro regions when spatially allocating new associative fear memories.

Spatial allocation of activated neurons at another rostrocaudal location (Bregma −3.24)

We chose the location for an additional mapping site (−3.24) that was proximal to our original analysis (−3.36) to retain stereotaxic alignment between brains.

PCA was conducted on 25 subjects (from all four conditions) and 44 bins (1,21 neurons) from the LAd (Paired 77.1 ± 7.7; Unpaired 44.8 ± 9.8; Shock 39.5 ± 5.3; Naïve 31.4 ± 3.9). PCA extracted ten SCs. Statistical analysis of all SCs revealed a single SC (SC2) whose factor score differed significantly among conditions (one-way ANOVA, $F[3, 21] = 6.4$; $p = 0.003$). Importantly, the loading values for SC2 corresponded with the difference in spatial distribution of pMAPK$^+$ neurons across experimental conditions, as depicted by the density maps (Fig. 6). A subsequent Bonferroni post-hoc test on the SC2 factor scores revealed significantly greater scores for subjects in the Paired group relative to those in the Shock ($p = 0.005$) and Box-alone ($p = 0.01$) conditions. There was a trend toward statistically significant difference in the Paired versus Unpaired condition ($p = 0.065$). Like the original spatial analysis conducted at −3.36 Bregma, this result confirms that a stable spatial allocation of pMAPK$^+$ neurons distinguished the experimental conditions. A statistical comparison of the factor scores for the remaining SCs (SC 1 and 3–10) failed to yield another spatial component that could account for any other source of variability in the spatial distribution of pMAPK$^+$ neurons between experimental conditions. This result indicates that the spatial pattern of pMAPK$^+$ neurons extracted in SC2 was unique to Paired auditory fear conditioning. The scores for SC1 and SC2 significantly correlated ($r = 0.58$, $p = 0.002$) (Fig. 7). Together, these statistical measures indicate that the spatial pattern of activated neurons in the LAd that was associated with SC1 and SC2 spanned at least 120 μm along the rostrocaudal axis.

Cytoarchitecture of principal neurons in the amygdala

Dual-labeling immunofluorescence

Analysis of the LA and B nuclei of the amygdala revealed that the majority of pMAPK fluorescent positive neurons

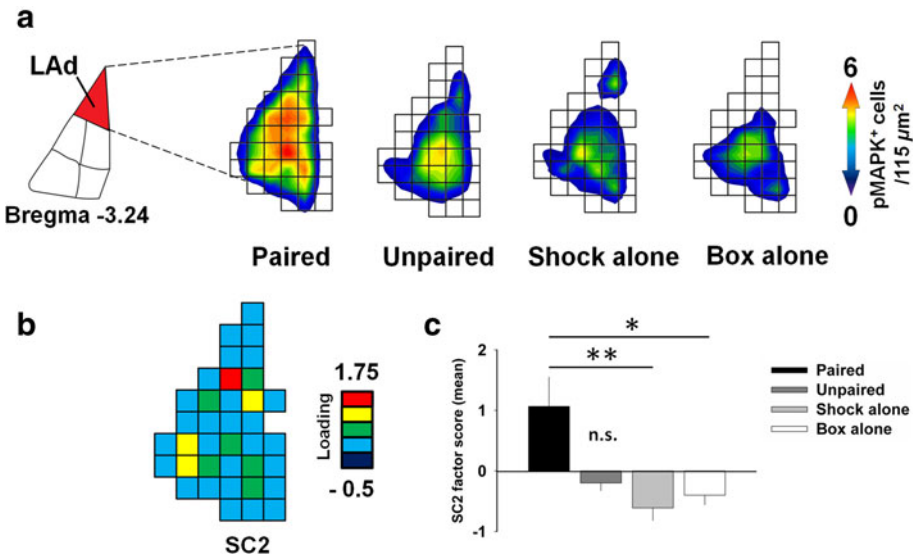

Fig. 6 PCA conducted at an additional coronal plane (Bregma −3.24) revealed another topography of neurons in the LAd that was unique to the encoding of an auditory Pavlovian fear conditioning. **a** Depiction of the spatial resolution and geometry of the matrix used in generating the density "heat" maps and PCA on the LAd at Bregma −3.24. The spatial resolution of the heat maps and the loading matrix was identical (115 μm^2). **b** Of the ten SCs extracted by PCA, the pattern of loading values associated with SC2 best discriminated the most prominent difference in the spatial distribution pMAPK$^+$ neurons between experimental conditions. **c** The mean scores for SC2 were significantly greater in the Paired group relative to the Shock-alone ($p = 0.005$) and Box-alone ($p = 0.01$) conditions (Bonferroni post hoc). The difference in the mean SC2 scores between the Paired and Unpaired conditions approached statistical significance ($p = 0.065$)

were co-localized with CaMKII fluorescent positive neurons (86.7 %, $n = 184/212$, sections = 15, rats $n = 2$, Bregma −2.04 to −3.60) (Fig. 8). Of the entire population of pMAPK$^+$ neurons studied, 3.7 % ($n = 8/212$) could not be accurately identified as either co-localized with CaMKII or not co-localized. The remaining 9.4 % ($n = 20/212$) of the pMAPK$^+$ population of neurons studied were visually determined to not be co-localized with CaMKII$^+$. These neurons are presumably GABAergic (McDonald et al. 2002), because the peak of pMAPK activation following conditioned fear learning has previously been localized to neurons and not glia (Di Benedetto et al. 2009). Overall, these results show that the majority (86.7 %) of pMAPK expression in the amygdala following fear conditioning is localized to the principal cell type (Fig. 8).

Mapping principal neurons in the LA and B

Next, CaMKII immuno-positive (CaMKII$^+$) neurons were mapped from a single section that was stringently matched using the LV as an anatomical landmark (see above). The use of single section for CaMKII$^+$ neuron mapping that was identical to the section chosen for pMAPK mapping aided in the accuracy of comparisons.

To visualize the spatial distribution of CaMKII$^+$ neurons across amygdala nuclei, density heat maps were generated using procedures identical to those described previously. A visual inspection of the maps clearly revealed variability in the density of CaMKII$^+$ neurons across amygdala nuclei (Fig. 9), an observation consistent with a previous report (McDonald et al. 2002). This finding was supported by a statistical comparison of CaMKII$^+$ neuron density among nuclei (one-way ANOVA; $F[4, 15] = 8.8$; $p = 0.001$). A subsequent paired t test revealed a greater density of CaMKII$^+$ neurons in the LAd relative to LAvm ($p = 0.03$), BLa ($p = 0.013$), and BLp ($p = 0.0004$). Because the alpha subunit of CaMKII is restricted to principal neurons in the amygdala (McDonald et al. 2002), the present results indicate variability in the density of principal neurons across LA and B nuclei, with greater density in the LAd relative to the ventral LA and B nuclei of the amygdala.

Determining the interdependence of the topography of pMAPK$^+$ and CaMKII$^+$ neurons in the amygdala at 115 μm^2 spatial resolution

Principal components analysis was applied to the pMAPK$^+$:CaMKII$^+$ data set to evaluate whether LAd principal cytoarchitecture determined the pattern of functionally active neurons observed following Pavlovian auditory fear conditioning. We reasoned that if spatial patterning of pMAPK$^+$ neurons is determined by the anatomical distribution of principal neurons then it would be

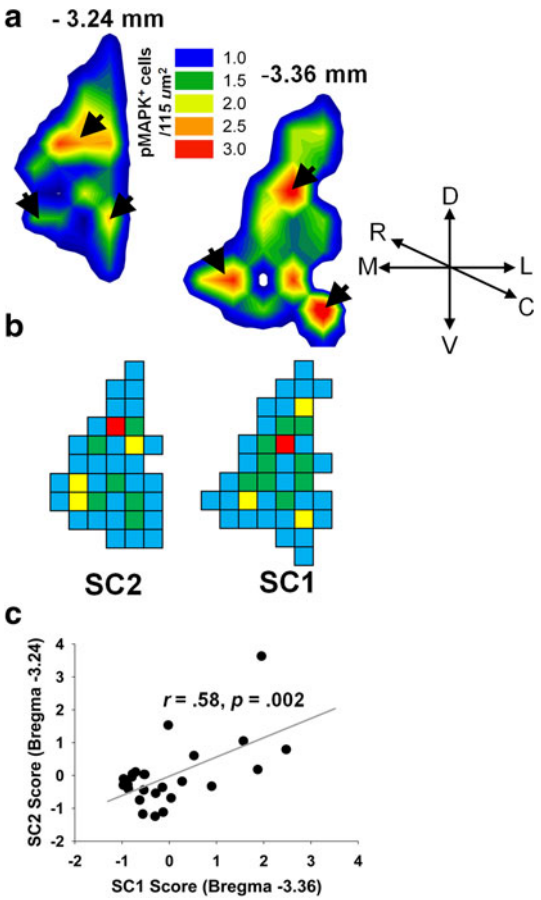

Fig. 7 The spatial allocation of neurons encoding a cued fear memory was highly consistent across two rostrocaudal locations in the LAd. **a** The spatial distribution of pMAPK neurons (115 μm^2 resolution), as depicted by difference maps, was similar across two rostrocaudal locations (Bregma −3.24 and −3.36) in the LAd. The difference maps were created by subtracted the mean number of neurons across all control groups from the Paired group. *Arrowheads* indicate regions of similarity **b** PCA extracted two SCs (1 and 2) that were specific to cued fear conditioning and contained a highly consistent pattern of loading values. **c** The scores for SC1 and SC2 significantly correlated ($r = 0.58$), suggesting a degree of stability in the prominence of the particular pattern associated with SC1 and SC2 across the rostrocaudal axis of individual animals

expected that the spatial distribution pMAPK$^+$:CaMKII$^+$ values would be relatively homogenous. However, if the anatomical distribution of principal neurons was inconsistent with the spatial pattern of pMAPK$^+$ neurons, then heterogenous pMAPK$^+$:CaMKII$^+$ values would be expected. To test this question, we applied PCA to pMAPK$^+$:CaMKII$^+$ values in each bin. The pMAPK$^+$:CaMKII$^+$ ratio values in bins were the dependent variables in the PCA. The spatial resolution of the matrix used for binning pMAPK$^+$ and pMAPK$^+$:CaMKII$^+$ values was identical, and therefore, direct comparison could be made between the topographic maps.

The spatial organization of pMAPK$^+$ neurons does not reflect the intrinsic cytoarchitecture

Principal components analysis on the LAd produced ten spatial components. ANOVA on all spatial components revealed a single spatial component (SC1) whose factor score differed significantly among experimental conditions ($F_{3,21} = 20.2$; $p = 0.000002$). The pattern of loading values associated with SC1 closely corresponded with the difference in the pattern of pMAPK$^+$:CaMKII$^+$ ratio values across experimental conditions as depicted in the topographic density maps (Fig. 10). A subsequent post-hoc test on the factor scores for SC1 revealed significantly greater scores for the Paired group relative to those in the Unpaired ($p = 0.00003$), Shock-alone ($p = 0.00002$) and Box-alone ($p = 0.00002$) conditions. There were no significant differences detected between any combination of the Unpaired, Shock and Naïve conditions. We also statistically compared the scores associated with the remaining spatial components (2–10) extracted by the PCA (Fig. 10). Importantly, we found that none of the remaining extracted spatial components was found to discriminate the experimental conditions. For visualization purposes, we projected the components scores for individual subjects

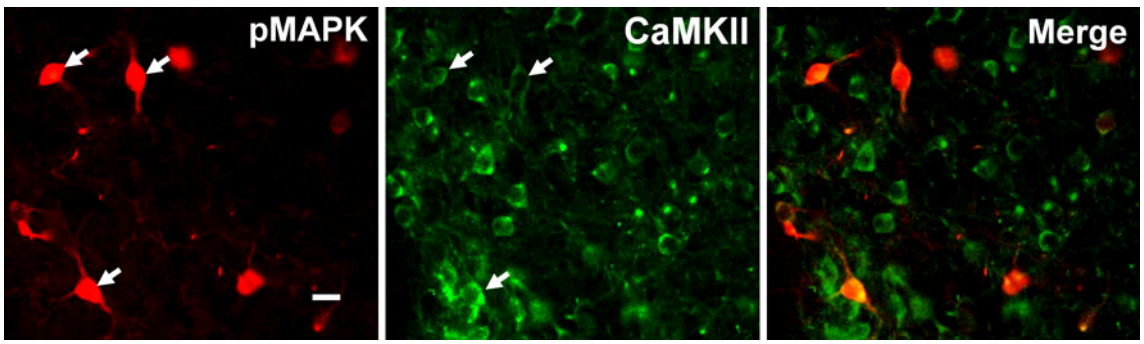

Fig. 8 pMAPK/CaMKII dual-labeled immunofluorescence. The majority of pMAPK immunofluorescent-labeled cells (*white arrowheads*) in the LA and B amygdala visualized 60 min following the acquisition of fear conditioning were simultaneously labeled with CaMKII (86.7 %). This result suggests that the peak of pMAPK expression following fear learning is predominately localized to principal neurons in the amygdala. ×20 magnification. *Scale bar* represents 15 μm

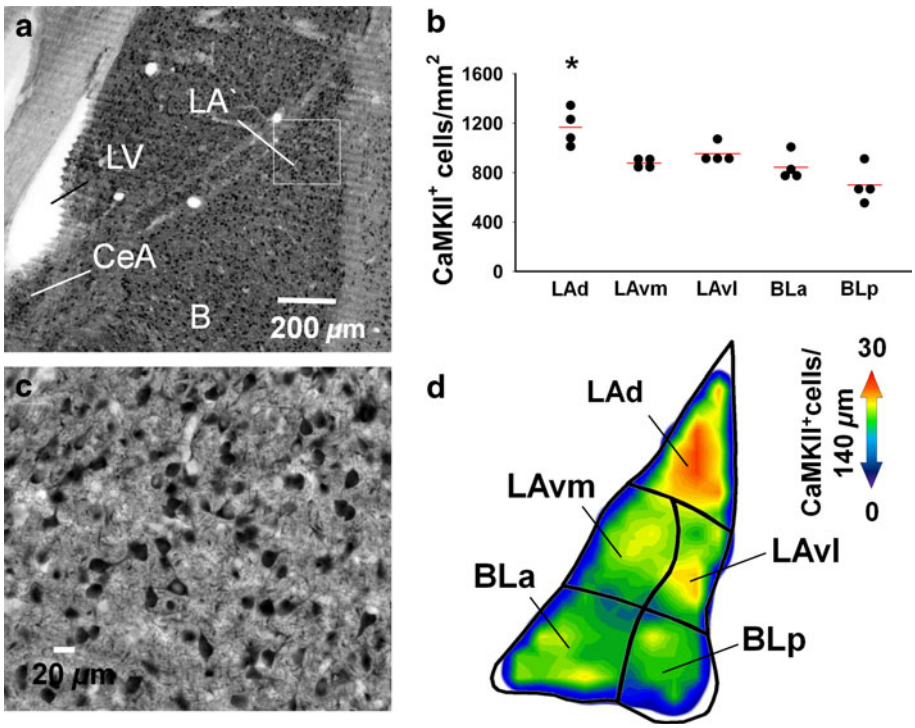

Fig. 9 Cytoarchitecture of CaMKII immunolabeled neurons in the LA and B nuclei of the amygdala. **a** Representative photomicrograph of a CaMKII immunohistochemical-processed section showing the various subnuclei of the amygdala and CaMKII$^+$ neurons at ×4 magnification (*left panel*), and ×20 magnification (*right panel*). **b** Dot density plot of CaMKII labeled neurons for all amygdala nuclei sampled in four subjects. CaMKII density for the LAd was greater compared to the ventral LA and B nuclei (paired *t* test). *Red line* depicts the mean. **c** Spatial density "heat" map depicting the distribution of CaMKII labeling for the LA and B nuclei at −3.36 Bregma (140 μm^2 spatial resolution). *Asterisk* denotes $p < 0.05$. *LAd* dorsolateral amygdala, *LAvm* ventromedial division, *LAvl* ventrolateral division, *BLa* anterior basolateral amygdala, *BLp* posterior basolateral amygdala

onto a two-dimensional axis (Fig. 10). Together, these results indicate that the spatial pattern of pMAPK$^+$ neurons associated with SC1 was unique to the encoding of an auditory fear conditioned memory. Furthermore, heterogeneity in the distribution of pMAPK$^+$:CaMKII$^+$ values throughout the LAd indicates that a large element of the functional map of pMAPK$^+$ neurons that forms following the acquisition auditory fear conditioning is independent of the underlying cytoarchitecture of principal neurons in the LAd. PCA was conducted on the pMAPK$^+$:CaMKII$^+$ values for the remaining amygdala nuclei. Results show that there were no other patterns extracted by PCA that could discriminate all experimental conditions.

A comparison of loading values for SC1 from the pMAPK$^+$ analysis with those from the pMAPK$^+$:CaMKII$^+$ analysis revealed that, while the overall pattern of loading values was similar between analyses, there was the appearance of a ventral shift in the "strength" of the loading values. That is, the pattern depicted in both the density maps and loadings values for SC1 confirmed a greater pMAPK$^+$:CaMKII$^+$ proportion of neurons located at the ventral portion of the LAd. There remained a relatively high proportion of pMAPK$^+$:CaMKII$^+$ neurons in a superior quadrant of the LAd, a finding consistent with previous work (Bergstrom et al. 2011). A comparison of pMAPK$^+$:CaMKII$^+$ values between experimental conditions for the bins with the greatest loading values (multiple comparison analyses; Supplemental results) confirmed a greater proportion of pMAPK$^+$:CaMKII$^+$ neurons for the Paired group in identical locations to those found for the pMAPK$^+$ map (Bin 13, 27, 36 and 7; Fig. 4). We conclude that, most likely, some portion of the pMAPK$^+$ map following Pavlovian fear conditioning is influenced by the intrinsic distribution of principal neurons. At the same time, the close resemblance of the pMAPK$^+$:CaMKII$^+$ map with the pMAPK$^+$ map suggests a high degree of independence from the cytoarchitecture.

Overall, PCA uncovered a stable spatial pattern of pMAPK$^+$ neurons in the LAd that was (1) unique to brains encoding Pavlovian auditory fear conditioning and (2) independent from the cytoarchitecture of the LAd.

Discussion

Determining how specific memories are allocated in neural networks is essential to understanding memory encoding in the brain. The stability of memory allocation across

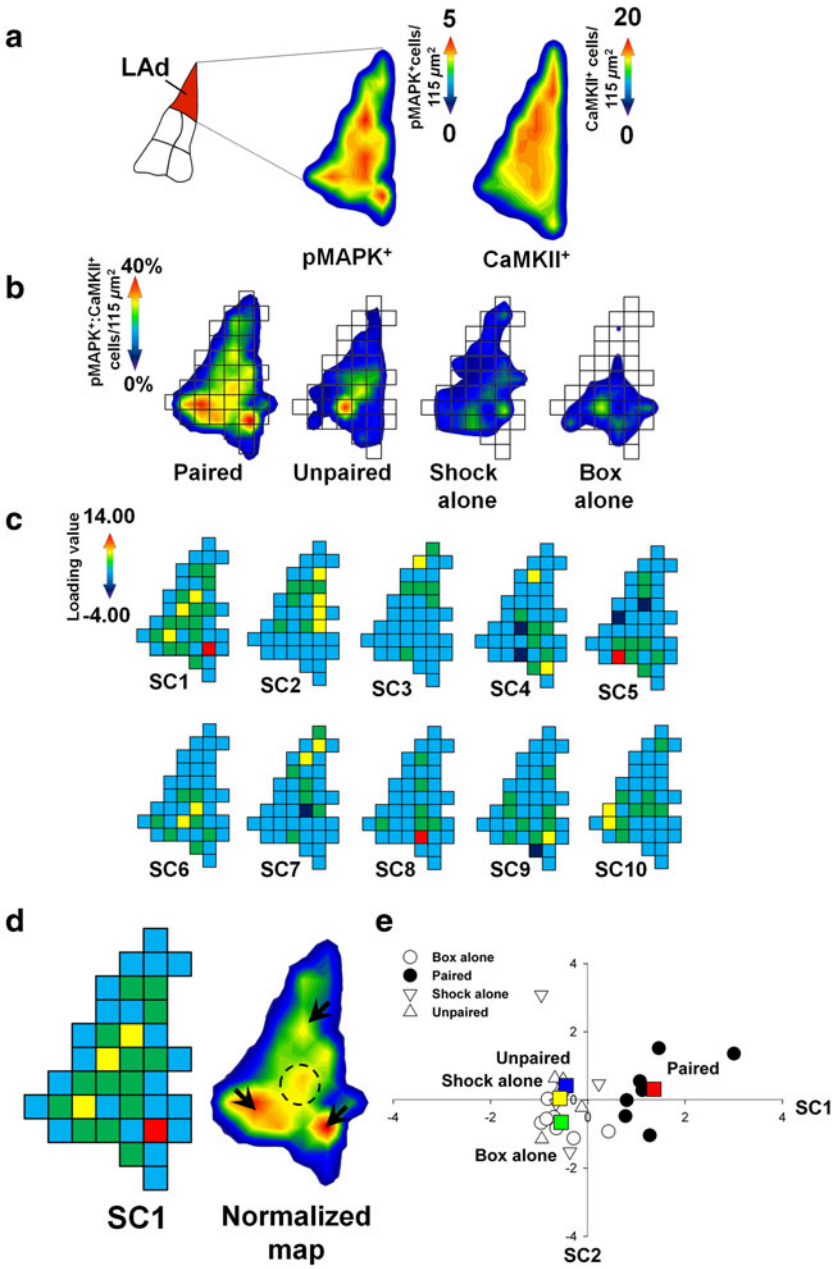

Fig. 10 A unique spatial organization of pMAPK$^+$ neurons following the acquisition of auditory fear conditioning is independent of intrinsic cytoarchitecture in the LAd. **a** Density "heat" maps of the LAd from the Paired experimental condition depicting the distribution of pMAPK$^+$ neurons (*left panel*) and CaMKII$^+$ neurons (*right panel*). The spatial resolution was identical between groups (115 μm^2). **b** Depiction of the spatial resolution and geometry of the matrix used for PCA on the normalized pMAPK values in the LAd. **c** PCA extracted ten spatial components (SCs). **d** Of the ten SCs extracted by PCA, only the pattern of loading values associated with SC1 adequately discriminated the difference in the normalized pMAPK values between experimental conditions. The *arrowheads* indicate regions of greatest difference between groups. **e** To illustrate how the SCs segregated the conditions along the first two spatial components (SC 1 and SC2), we projected the SC scores for individual subjects onto a two-dimensional axis. The SC1 scores for the Paired condition were significant different from the Unpaired ($p = 0.00003$), Shock-alone ($p = 0.00002$) and Box-alone ($p = 0.00002$) conditions, indicating that SC1 represented a pattern of normalized pMAPK values that was specific to the acquisition of auditory fear conditioning

individual brains is of particular interest. In this study, we hypothesized that a newly formed fear memory would be associated with a unique and stable spatial organization of activated neurons in the amygdala and that this map would be a function of memory formation itself and not primarily determined by the intrinsic cytoarchitecture of principal neurons. To address these hypotheses, we applied PCA to extract patterns from a highly complex population of pMAPK$^+$ neurons from the lateral and basal subnuclei of the amygdala. Results from PCA supported our prediction, showing that a stable spatial pattern of pMAPK$^+$ neurons in the LAd was unique to those encoding auditory Pavlovian fear conditioning. The cytoarchitecture of principal neuronal density could not account for the geometry of the map, indicating for the first time that spatial organization of neurons encoding fear memory is a function of memory formation itself. Consistent spatial patterning across brains was not evident for any of the ventral LA (LAvl and LAvm) or B (BLa and BLp), suggesting a localized topographical organization for cued fear memory formation in the LAd. This result is in agreement with a previous study showing that the medial amygdala was not associated with a topographic map for cued fear conditioning (Bergstrom et al. 2011). Spatial analyses conducted at another coronal plane (Bregma −3.24) (Fig. 6) revealed another functional map specific to cued fear conditioning, with topographic

measurements highly consistent with the original map analyzed at Bregma −3.36 (Fig. 7). Overall, these findings support evidence that fear memory encoding in the LAd is non-random and provide additional insight into the spatial allocation of the engram. Further, these results suggest that the formation of an auditory-conditioned fear memory is allocated across different brains to a spatially stable and autonomous network of neurons in the LAd that is independent of the intrinsic cytoarchitecture.

A functional map represents cued fear conditioning

Examination of the spatial maps from the LA and B nuclei revealed the most common location for $pMAPK^+$ neurons after Pavlovian fear conditioning was an area in the inferior LAd (Figs. 2, 4), an observation previously described in experiments using qualitative (Radwanska et al. 2002; Schafe et al. 2000) and quantitative measures (Bergstrom et al. 2011). In addition, this location was observed following long-term potentiation (LTP)-inducing stimulation (Schafe et al. 2008). A significant challenge in the present study was to statistically segregate commonly activated ("background") neurons from neurons specific to encoding auditory fear conditioning across all LA and B subnuclei. PCA revealed a single spatial component (SC1) with an activation pattern containing at least two discrete areas in the LAd with a high density of $pMAPK^+$ neurons that were unique to those encoding auditory Pavlovian fear conditioning. The most prominent regions were anatomically localized to the inferior and superior LAd (Fig. 4). The LAvl was another prominent location in the amygdala that contained a greater number of $pMAPK^+$ neurons specific to associative fear learning (Fig. 2).

Contextual fear memory formation is not represented by a functional map

The amygdala is a heterogeneous structure composed of anatomically and functionally distinct nuclei (Pitkänen 2000; McDonald 2003). It is widely understood that amygdala afferents related to the generation of associative fear memories terminate along two major subdivisions of the amygdala: the lateral (LA) and basal (B) nuclei. While plasticity at synapses of neurons in the LA is critical to the formation of cued fear memories (Blair et al. 2001; Schafe et al. 2005; Romanski et al. 1993; Quirk et al. 1995), the B nucleus, possessing anatomical and functional interactions with the hippocampus (Pitkänen 2000), has been more closely associated with processing of contextual fear memories (Nader et al. 2001; Calandreau et al. 2005; Reijmers et al. 2007; Fanselow and LeDoux 1999; Onishi and Xavier 2010; Phillips and LeDoux 1992; Kim and Fanselow 1992). Therefore, we reasoned that a unique spatial organization of activated neurons might be specific to contextual fear and that this map might be located in the B nucleus. In contrast to our hypothesis, contextual fear was not found to be associated with either increased density or a systematic spatial pattern of $pMAPK^+$ neurons in the B nucleus, or any of the other LA subregions (LAd, LAvl, LAvm). A lack of pMAPK labeling in the LA following contextual fear conditioning has been reported previously (Schafe et al. 2000). Together, these results imply that contextual fear was not spatially organized in the amygdala, at least not for neurons expressing pMAPK in the coronal plane chosen for analyses. A possibility remains for the existence of contextual fear memory maps located outside the coronal plane analyzed in the present study. Another possibility is that more subtle topographic differences relating to encoding contextual fear memory were not detected at the spatial resolution (115 μm^2) of our analysis. A final possibility is that pMAPK may not be a reliable marker for contextual fear conditioning in amygdala (LA and B nuclei), but is a marker elsewhere. This possibility is supported by evidence showing that an injection of a MAPK inhibitor into the ventricles disrupted contextual fear memory consolidation (Schafe et al. 1999). Recent work identified a discrete neuronal population localized to the LAvl that were specifically activated during the acquisition of contextual fear conditioning (Trogrlic et al. 2011; Wilson and Murphy 2009). Using the analytic and molecular methods here (PCA and pMAPK, respectively), we did not uncover a similar pattern.

Spatial analytics for studying the topographical organization of neuronal populations

For this series of experiments and a previous one (Bergstrom et al. 2011), we developed a novel application of PCA that was used to reduce a complex spatial distribution of neurons in the amygdala into a simpler set of uncorrelated spatial components. In the present study, the matrix self-organized based on the *XY* coordinates of mapped neurons. This technique eliminated any potential bias resulting from ad-hoc matrix construction. In addition, all conclusions drawn from PCA were derived exclusively from (1) multiple comparisons analyses (Bonferroni corrected) on the raw neuron number matrix, (2) MANOVA on all component scores and (3) a visual comparison of the PCA loading matrix with the corresponding topographical heat maps. To make the most accurate comparisons possible, we scaled the spatial resolution and geometry of the density maps to match the matrix developed for PCA. The PCA approach described in this paper provides a new statistical tool for deciphering and quantifying complex spatial patterning of cells and has application across all types of tissue, especially the spatial allocation of memory.

The PCA allowed us to make a secondary analysis of the degree of plasticity of associative memory activated neurons located in discrete micro regions of the LAd (Fig. 4). These micro regions (115 μm^2 each) possessed a significant degree of associative learning-induced neuronal plasticity (157 % increase) compared with the plasticity distributed across the whole LAd (40 % increase), and accounted for at least 37 % of neurons encoding CS and US pairings (Fig. 4). Thus, we can conclude from these data that a spatial component of the fear memory was allocated to highly plastic micro regions of the LAd. Overall, the present study provides the first quantitative measures for the spatial distribution of neurons allocated to a specific fear memory trace in the LAd.

Quantitative brain alignment

Spatial organization is reflected by the degree of consistency of a particular pattern of neurons across different brains. To establish consistency, comparisons must be conducted at an equivalent location in space. This is a significant technical challenge fundamental to the study of localization of brain function. Here, we devised a novel approach to stereotaxic alignment across individual brains. We used the rapidly diverging rostral-most entrance of the lateral ventricle as a reliable anatomical reference point (−3.36 mm Bregma) (Paxinos and Watson 2007). Morphometrics derived from in vitro (histology) and in vivo (MRI) digital reconstructions verified that the rapid change in shape of the LV was not an artifact of histological processing (Fig. 1). Combining these techniques enabled quantitative identification of matched amygdala regions from individual brains. Low variability in brain alignment enhances the likelihood of finding organized neuronal patterning. At increasing distances away from the anatomical reference point, variability in brain alignment also increases which may prevent the emergence of neuronal patterning. For this reason, additional mapping was conducted at a location that was relatively proximal (Bregma −3.24) to the LV entrance (Bregma −3.36) (Figs. 6, 7). Future studies of neural patterning, at distal locations outside Bregma −3.24 to −3.36, will require new anatomical landmarks or novel methodology for aligning serial brain sections in common stereotaxic space.

Factors determining the cellular allocation of fear conditioning in the LAd

Understanding precisely where specific memories are allocated, and the degree of consistency for specific memories across individuals, is a major goal of neuroscience. One key determinant for memory allocation is the intrinsic micro-organization of the circuit. Using dual-labeling immunofluorescence, we found that 86.8 % of pMAPK expressing neurons were co-localized with CaMKII-labeled neurons (Fig. 8). These results indicate that the peak of pMAPK expression following fear learning is predominately localized to principal neurons in the LAd, although there is a possibility that other cell types might also express pMAPK following learning. Next, we controlled for the role of local density of principal neuron cytoarchitecture by quantifying the spatial relationship between principal ($CaMKII^+$) and $pMAPK^+$ neurons at 115 μm^2 spatial resolution. All topographic measurements of the LAd, both for pMAPK and CaMKII immuno-stained neurons, were conducted at 115 μm^2 spatial resolution. The topographic relationship between $pMAPK^+$ and $CaMKII^+$ neuronal density at sub-115 μm^2 spatial resolution remains unknown. Overall, these data indicate that a functional network unique to Pavlovian fear conditioning and independent from the local neuronal density of principal neurons can be measured in the LAd (Fig. 9).

A second organizing factor for memory allocation of Pavlovian fear is the distribution of CS and US containing afferents along the dorsoventral axis. The principles governing the organization of these afferents in the LA and B are not yet fully understood. However, classic anatomical studies have shown a broad distribution of sensory thalamic and sensory cortex distribution to the LA (Pitkänen 2000; Johnson and Ledoux 2004; McDonald 1998; Romanski et al. 1993; Doron and Ledoux 1999). The possibility for a tonotopic map in the LA is of particular interest (LeDoux et al. 1991). It is feasible that the spatial map identified in the current study may represent a tonotopic distribution that follows the dorsoventral axis. Future studies on different sensory modalities (visual or olfactory) and auditory frequencies will help to answer this question. The current data establish a functional memory map as independent of LAd principal neuron density.

A third organizing factor for the cellular allocation of Pavlovian fear is the rostrocaudal distribution of CS and US containing afferents. Mapping was conducted in the caudal portion of the amygdala (Bregma −3.24 and −3.36). Tract-tracing studies of extrinsic and intrinsic connectivity show the amygdala receives auditory and nociceptive information from both cortical and thalamic afferents (McDonald 1998; LeDoux et al. 1990b, 1991; Bernard et al. 1993; Pitkänen 2000). A visual inspection of these data clearly shows the caudal amygdala receives a substantial portion of these projections. If we assume that associative fear memory is allocated according to the relevant connectivity along the rostrocaudal axis, we predict a corresponding topography of fear memory storing cells. Finer-scale mapping of afferent connectivity in the amygdala might reveal areas where fear memory is, or is not, housed based on the rostrocaudal gradient of sensory afferents.

The existence of a local excitatory network in the LAd is another organizing factor that may help to explain the source of organization among functionally active neurons following fear learning (Johnson and LeDoux 2004, 2010). Both in vitro and in vivo experiments have revealed evidence for a recurrent network, spatially organized in the superior and inferior LA, which bound temporally incongruent thalamic and cortical afferent signals to facilitate associative learning (Johnson et al. 2008, 2009). The finding of a local excitatory network in the LAd is consistent with another experiment showing two different neuronal populations in the LAd, anatomically organized to the superior and inferior LAd, that were engaged at different times during the course of fear learning (Repa et al. 2001). An important question remains as to whether the neurons from the present study belong to the same or different local excitatory network as that described by Repa et al. (2001) and Johnson et al. (2008).

Conclusions

We found a spatially organized topography of neurons in the LAd that was specific to Pavlovian fear conditioning. The topography was independent from intrinsic principal neuron density, with micro regions containing a high degree of learning-induced plasticity. Stability in the spatial patterning of functionally active neurons across individual brains suggests that a deterministic, or non-random, process may control how neurons involved in memory formation are allocated. These data provide an important step toward understanding organizing principles of the engram.

Acknowledgments We are very grateful to Dr Robert Ursano and the Center for the Study of Traumatic Stress (CSTS) for support. We thank Dr Alex McDonald for advice on the CaMKII antibody and Dr Jennifer McGuire for advice on immunofluorescence. Supported by Grants USU #NW188NW and USU #NWI88NZ.

References

Bergstrom HC, McDonald CG, French HT, Smith RF (2008) Continuous nicotine administration produces selective, age-dependent structural alteration of pyramidal neurons from prelimbic cortex. Synapse 62(1):31–39

Bergstrom HC, McDonald CG, Johnson LR (2011) Pavlovian fear conditioning activates a common pattern of neurons in the lateral amygdala of individual brains. PLoS ONE 6(1):e15698

Bernard JF, Alden M, Besson JM (1993) The organization of the efferent projections from the pontine parabrachial area to the amygdaloid complex: a *Phaseolus vulgaris* leucoagglutinin (PHA-L) study in the rat. J Comp Neurol 329(2):201–229

Blair HT, Schafe GE, Bauer EP, Rodrigues SM, LeDoux JE (2001) Synaptic plasticity in the lateral amygdala: a cellular hypothesis of fear conditioning. Learn Mem 8(5):229–242

Calandreau L, Desmedt A, Decorte L, Jaffard R (2005) A different recruitment of the lateral and basolateral amygdala promotes contextual or elemental conditioned association in Pavlovian fear conditioning. Learn Mem 12(4):383–388

Davis M (1992) The role of the amygdala in fear and anxiety. Annu Rev Neurosci 15:353–375

Davis S, Laroche S (2006) Mitogen-activated protein kinase/extracellular regulated kinase signalling and memory stabilization: a review. Genes Brain Behav 5(Suppl 2):61–72

de Smith MJ, Goodchild MF, Longly PA (2009) Geospatial Analysis. Matador, Leicester

Di Benedetto B, Kallnik M, Weisenhorn DM, Falls WA, Wurst W, Holter SM (2009) Activation of ERK/MAPK in the lateral amygdala of the mouse is required for acquisition of a fear-potentiated startle response. Neuropsychopharmacology 34(2):356–366

Doron NN, Ledoux JE (1999) Organization of projections to the lateral amygdala from auditory and visual areas of the thalamus in the rat. J Comp Neurol 412(3):383–409

Duvarci S, Nader K, LeDoux JE (2005) Activation of extracellular signal-regulated kinase- mitogen-activated protein kinase cascade in the amygdala is required for memory reconsolidation of auditory fear conditioning. Eur J Neurosci 21(1):283–289

Fanselow MS (1980) Conditioned and unconditional components of post-shock freezing. Pavlov J Biol Sci 15(4):177–182

Fanselow MS, LeDoux JE (1999) Why we think plasticity underlying Pavlovian fear conditioning occurs in the basolateral amygdala. Neuron 23(2):229–232

Han JH, Kushner SA, Yiu AP, Cole CJ, Matynia A, Brown RA, Neve RL, Guzowski JF, Silva AJ, Josselyn SA (2007) Neuronal competition and selection during memory formation. Science 316(5823):457–460

Han JH, Kushner SA, Yiu AP, Hsiang HL, Buch T, Waisman A, Bontempi B, Neve RL, Frankland PW, Josselyn SA (2009) Selective erasure of a fear memory. Science 323(5920):1492–1496

Herry C, Trifilieff P, Micheau J, Luthi A, Mons N (2006) Extinction of auditory fear conditioning requires MAPK/ERK activation in the basolateral amygdala. Eur J Neurosci 24(1):261–269

Johnson LR, Ledoux JE (eds) (2004) The anatomy of fear: microcircuits of the lateral amygdala. In: Fear and anxiety: the benefits of translational research. American Psychiatric Publishing, Inc, Washington, DC

Johnson LR, LeDoux JE (2010) Amygdala Microcircuits. In: Shepherd GM, Grillner S (eds) Handbook of brain microcircuits. Oxford University Press, Oxford

Johnson LR, Hou M, Ponce-Alvarez A, Gribelyuk LM, Alphs HH, Albert L, Brown BL, Ledoux JE, Doyere V (2008) A recurrent network in the lateral amygdala: a mechanism for coincidence detection. Front Neural Circuits 2:3

Johnson LR, Ledoux JE, Doyere V (2009) Hebbian reverberations in emotional memory micro circuits. Front Neurosci 3(2):198–205

Jolliffe IT (2002) Principal component analysis, vol 2. Wiley Online Library, New York

Kim JJ, Fanselow MS (1992) Modality-specific retrograde amnesia of fear. Science 256(5057):675–677

Lamprecht R, LeDoux J (2004) Structural plasticity and memory. Nat Rev Neurosci 5(1):45–54

LeDoux JE, Cicchetti P, Xagoraris A, Romanski LM (1990a) The lateral amygdaloid nucleus: sensory interface of the amygdala in fear conditioning. J Neurosci 10(4):1062–1069

LeDoux JE, Farb C, Ruggiero DA (1990b) Topographic organization of neurons in the acoustic thalamus that project to the amygdala. J Neurosci 10(4):1043

LeDoux JE, Farb CR, Romanski LM (1991) Overlapping projections to the amygdala and striatum from auditory processing areas of the thalamus and cortex. Neurosci Lett 134(1):139–144

Maren S, Fanselow MS (1996) The amygdala and fear conditioning: has the nut been cracked? Neuron 16(2):237–240

Maren S, Quirk GJ (2004) Neuronal signalling of fear memory. Nat Rev Neurosci 5(11):844–852

McDonald AJ (1984) Neuronal organization of the lateral and basolateral amygdaloid nuclei in the rat. J Comp Neurol 222(4):589–606

McDonald AJ (1998) Cortical pathways to the mammalian amygdala. Prog Neurobiol 55(3):257–332

McDonald AJ (2003) Is there an amygdala and how far does it extend? An anatomical perspective. Ann N Y Acad Sci 985:1–21

McDonald AJ, Muller JF, Mascagni F (2002) GABAergic innervation of alpha type II calcium/calmodulin-dependent protein kinase immunoreactive pyramidal neurons in the rat basolateral amygdala. J Comp Neurol 446(3):199–218

Nader K, Majidishad P, Amorapanth P, LeDoux JE (2001) Damage to the lateral and central, but not other, amygdaloid nuclei prevents the acquisition of auditory fear conditioning. Learn Mem 8(3):156–163

Nomura H, Nonaka A, Imamura N, Hashikawa K, Matsuki N (2011) Memory coding in plastic neuronal subpopulations within the amygdala. Neuroimage 60(1):153–161

Onishi BK, Xavier GF (2010) Contextual, but not auditory, fear conditioning is disrupted by neurotoxic selective lesion of the basal nucleus of amygdala in rats. Neurobiol Learn Mem 93(2):165–174

Pape HC, Pare D (2010) Plastic synaptic networks of the amygdala for the acquisition, expression, and extinction of conditioned fear. Physiol Rev 90(2):419–463

Paxinos G, Watson C (2007) The rat brain in stereotaxic coordinates, 6th edn. Elsevier Academic Press, London

Phillips RG, LeDoux JE (1992) Differential contribution of amygdala and hippocampus to cued and contextual fear conditioning. Behav Neurosci 106(2):274–285

Pitkänen A (2000) Connectivity of the rat amygdaloid complex. In: Aggleton JP (ed) The amygdala, 2nd edn. Oxford University Press, New York

Quirk GJ, Repa C, LeDoux JE (1995) Fear conditioning enhances short-latency auditory responses of lateral amygdala neurons: parallel recordings in the freely behaving rat. Neuron 15(5):1029–1039

Radley JJ, Farb CR, He Y, Janssen WG, Rodrigues SM, Johnson LR, Hof PR, LeDoux JE, Morrison JH (2007) Distribution of NMDA and AMPA receptor subunits at thalamo-amygdaloid dendritic spines. Brain Res 1134(1):87–94

Radwanska K, Nikolaev E, Knapska E, Kaczmarek L (2002) Differential response of two subdivisions of lateral amygdala to aversive conditioning as revealed by c-Fos and P-ERK mapping. NeuroReport 13(17):2241–2246

Reijmers LG, Perkins BL, Matsuo N, Mayford M (2007) Localization of a stable neural correlate of associative memory. Science 317(5842):1230–1233

Repa JC, Muller J, Apergis J, Desrochers TM, Zhou Y, LeDoux JE (2001) Two different lateral amygdala cell populations contribute to the initiation and storage of memory. Nat Neurosci 4(7):724–731

Romanski LM, Clugnet MC, Bordi F, LeDoux JE (1993) Somatosensory and auditory convergence in the lateral nucleus of the amygdala. Behav Neurosci 107(3):444–450

Rumpel S, LeDoux J, Zador A, Malinow R (2005) Postsynaptic receptor trafficking underlying a form of associative learning. Science 308(5718):83–88

Schafe GE, Nadel NV, Sullivan GM, Harris A, LeDoux JE (1999) Memory consolidation for contextual and auditory fear conditioning is dependent on protein synthesis, PKA, and MAP kinase. Learn Mem 6(2):97–110

Schafe GE, Atkins CM, Swank MW, Bauer EP, Sweatt JD, LeDoux JE (2000) Activation of ERK/MAP kinase in the amygdala is required for memory consolidation of pavlovian fear conditioning. J Neurosci 20(21):8177–8187

Schafe GE, Doyere V, LeDoux JE (2005) Tracking the fear engram: the lateral amygdala is an essential locus of fear memory storage. J Neurosci 25(43):10010–10014

Schafe GE, Swank MW, Rodrigues SM, Debiec J, Doyere V (2008) Phosphorylation of ERK/MAP kinase is required for long-term potentiation in anatomically restricted regions of the lateral amygdala in vivo. Learn Mem 15(2):55–62

Sweatt JD (2001) The neuronal MAP kinase cascade: a biochemical signal integration system subserving synaptic plasticity and memory. J Neurochem 76(1):1–10

Thomas GM, Huganir RL (2004) MAPK cascade signalling and synaptic plasticity. Nat Rev Neurosci 5(3):173–183

Trogrlic L, Wilson YM, Newman AG, Murphy M (2011) Context fear learning specifically activates distinct populations of neurons in amygdala and hypothalamus. Learn Mem 18(10):678–687

Wilensky AE, Schafe GE, LeDoux JE (1999) Functional inactivation of the amygdala before but not after auditory fear conditioning prevents memory formation. J Neurosci 19((24)):RC48

Wilson YM, Murphy M (2009) A discrete population of neurons in the lateral amygdala is specifically activated by contextual fear conditioning. Learn Mem 16(6):357–361